2017

Experimental Biomechanics of Trinucleid Fringe Pits (Trilobita)

Kirk Pearson
Oberlin College

Repository Citation

Pearson, Kirk, "Experimental Biomechanics of Trinucleid Fringe Pits (Trilobita)" (2017). *Honors Papers*. 184.
https://digitalcommons.oberlin.edu/honors/184

Experimental biomechanics of trinucleid fringe pits (*Trilobita*)

Kirk Pearson
Depts. of Geology and Biology, Oberlin College
Oberlin, OH 44074
kirk.pearson@oberlin.edu

Abstract

The morphometric uniqueness of the trinucleid family of fossil arthropods, known as the trilobites, has led to a considerable amount of attention in paleontology literature. In particular, the distinctive hourglass-shaped pits that dot their anterior have been the subject of debate for over a century. Though anatomically well understood, their function remains unknown. Many proposals have been suggested, including its use as a sieve for filter-feeding, a strong shield for defense, and a sensory mechanism to compensate for their blindness. Despite the wide range of speculations, no study has attempted to model these hypotheses experimentally. Flume experiments and mechanical strength tests using a tenfold scale, 3D-printed model of a trinucleid head suggest that the dominant theories for over a century, filter-feeding and skeletal strengthening, are not well supported. It is proposed that the results suggest that the pits are an ontogenetic signature that optimize the cephalon's growth to be maximal, providing trinucleids with an excellent mechanism for plowing through fine-grained silts and clays.

Introduction and Background

Anatomical Background

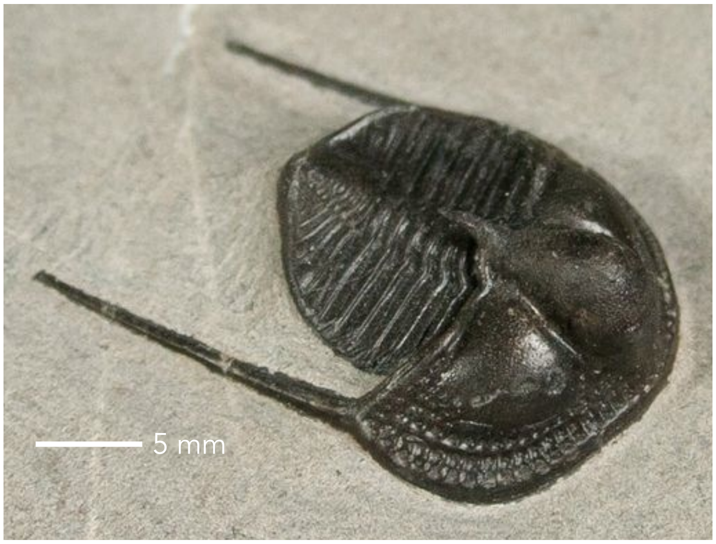

Fig I: *C. tesselatus*, a trinucleid, with a pitted cephalic fringe. (Image courtesy of Fossilera, 2015)

The asaphid trilobite family Trinucleidae were benthic dwellers in the Ordovician oceans (Campbell 1975). They are best characterized by their wide, perforated head shield located on the cephalon (Fig I). These perforations have traditionally been referred to as "fringe pits," or "pits," while the fringe has lent itself to a popular nickname for the family: "lace collar trilobites." Previous work has suggested that the fringe pits were added to the outermost layer of the cephalon, the cranidium, over several molts in a consistent order. The addition of new pits ceased before segment accretion ceased, meaning adult molts see no change in pit placement or arrangement (Whittington 1959, 1968; Chatterton et al. 1994). The glabella, the large, pear-shaped feature in the center of the cephalon (Fig II), expands towards the inner

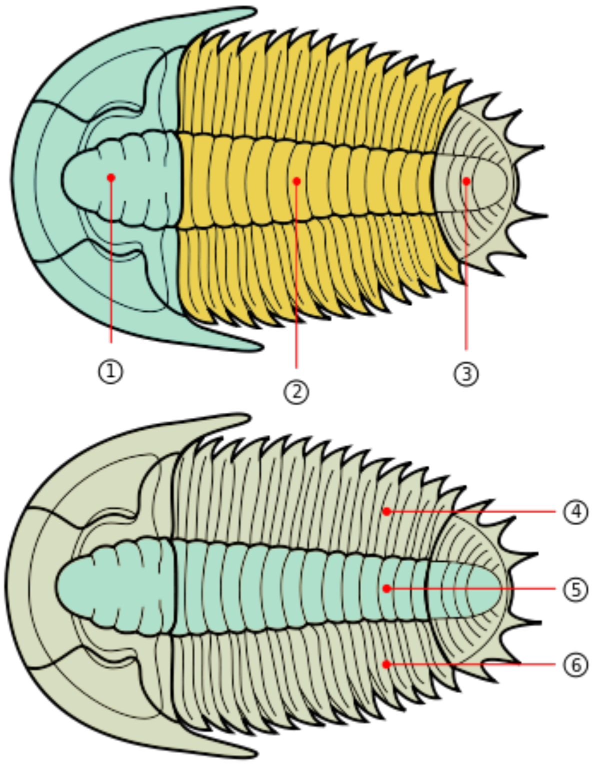

Fig II: An illustration of a generic trilobite showing its three major lateral divisions: the cephalon (1), the thorax (2), and the pygidium (3). The name "trilobite" comes from its three longitudinal lobes: the right pleural lobe (4), the axial lobe (5), and the left pleural lobe (6). (Graphic by Sam Gon III, 2011, Wikimedia Commons)

margin of the fringe where it makes contact with the innermost row of pits, which in turn extend toward the back and sides (posterolaterally) behind the cephalon. The pits increase in size as they move towards the periphery. In order to describe the location of any particular row of fringe pits, each is referred to by a list number: the "first internal list" describes the concentric arc of rings closest to the glabella, and increases as one moves outward (Hopkins and Pearson, 2016) Previous studies have shown that the number of pits in each list can change within ontogenetic stages and between variations of species (Whittington, 1968), noting that the specific placement of pits is not homologous across specimens.

In sagittal section, each pit resembles an hourglass (Fig IV) with a flared surface opening of approximately 400 µm narrowing to a funnel of 100 µm midway between the inner and outer surfaces of the fringe. A suture used for molting runs parallel to the surface of the fringe, bisecting the hourglass-shaped pits at their narrowest section—a

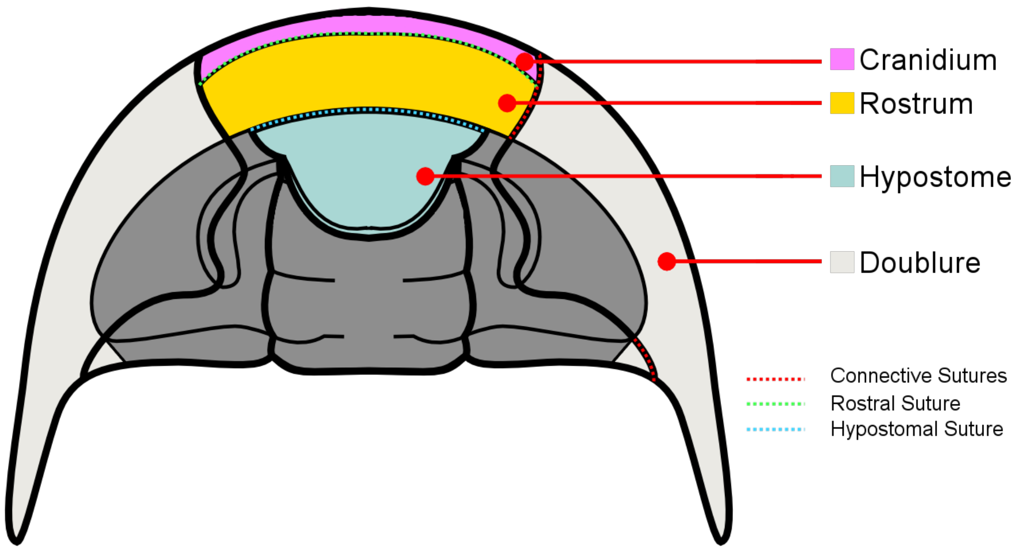

Fig III: An illustration of a trilobite cephalon, showing the ventral sutures. (Graphic by Sam Gon III, 2011, Wikimedia Commons) faint line defines this suture in Fig IV. A cross-section through the fringe shows several of these hourglasses with large, rounded vesicles in between them. These vesicles, as seen exposed in the photograph, are hollow and have been permineralized with calcite on all specimens (Fig V). This suggests the fringe was originally hollow and water filled. Taken as a whole, the structure resembles a series of interconnected tubes (the vesicles), arranged in a cross hatched pattern with the pits defining the sides of the tubes. While there is a possibility that these tubes were once channels for coelomic fluids, there is no remaining direct evidence for or against it.

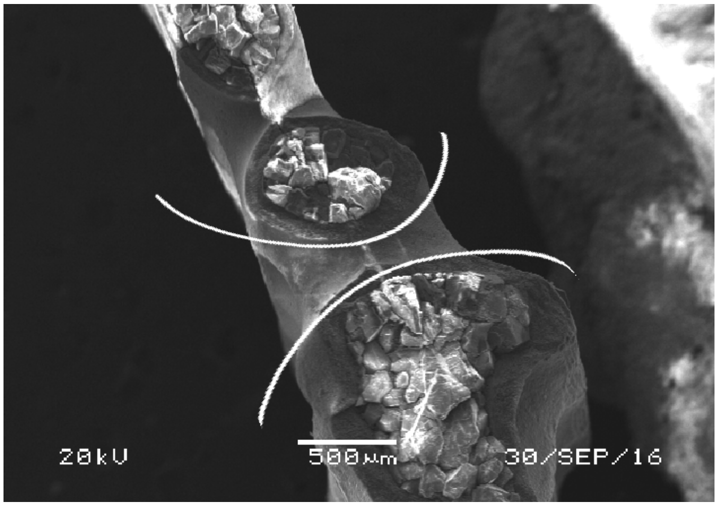

Fig IV: A sagittal section of the fringe of trinucleid *C. tesselatus.* White lines highlight the tapering hourglass shape of the pit. The vesicles are permineralized with calcite, whereas the aperture itself remains open.

While previous studies have described changes in the arrangement of these pits throughout ontogeny, their functional morphology remains hotly debated (Begg 1944, Hopkins and Pearson,

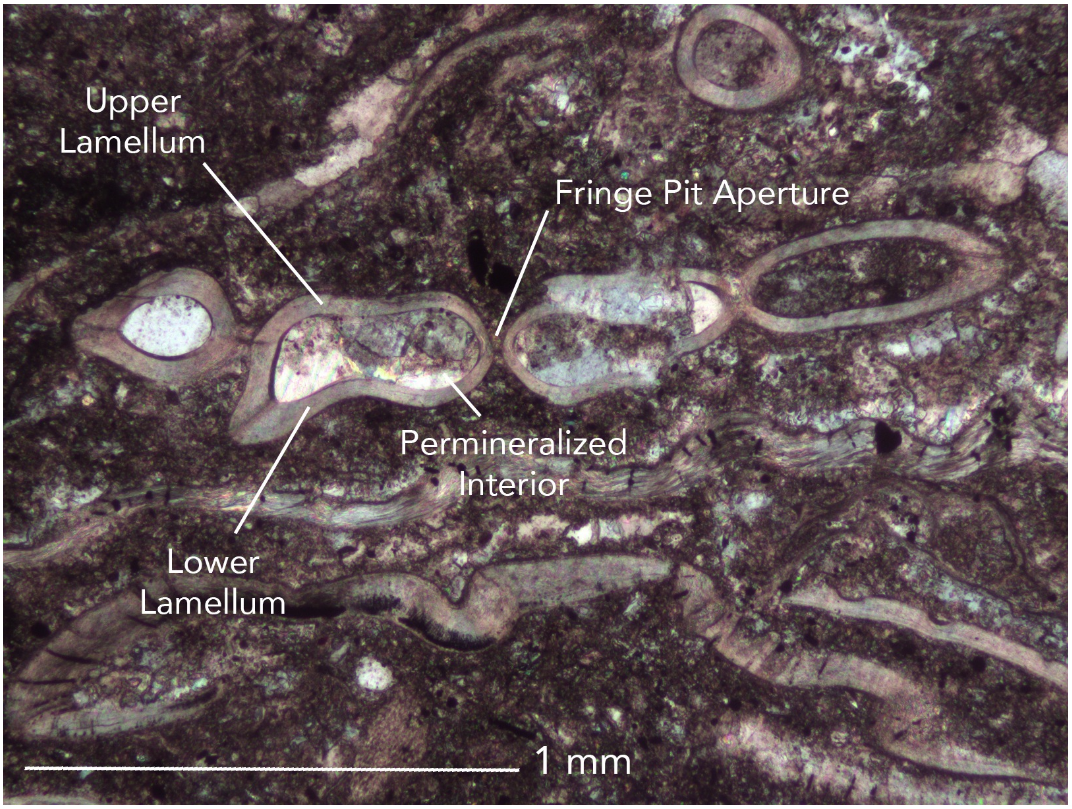

Fig V: A sagittal section of *C. tesselatus* in situ, showing the hourglass-shaped tapers with a permineralized interior and finer grained exterior.

2016). A usage of filter-feeding was proposed (Bergström 1969) and is the most commonly cited function to date. Owen (1980) upholds this hypothesis, noting that all trinucleids possess a vaulted cephalic chamber that could be used for filtration. Owen also argues that fringe pits found across all trinucleids are not analogous, and thus served the same function across all members of the family.

One such trinucleid, *Cryptolithus tesselatus* (Green 1832), is an especially common and famous member of the lace collar family (Fig VI). The multiple rows of variable-sized pits have been attributed to many functions, including the hypothetical uses of sediment filter-feeding (Begg 1944; Fortey and Owens 1999), burrowing (Bergström 1972, Osgood 1970), and exoskeleton strengthening (Osgood 1970). From fossil evidence and morphologic inference, *C. tesselatus* was a benthic feeder found in a very low energy depositional environment—a slow moving current that supports only fine-grained muds and clays. This study examines these hypotheses, along with several other morphologic inferences about the function of these pits along the anterior fringe of the cephalon.

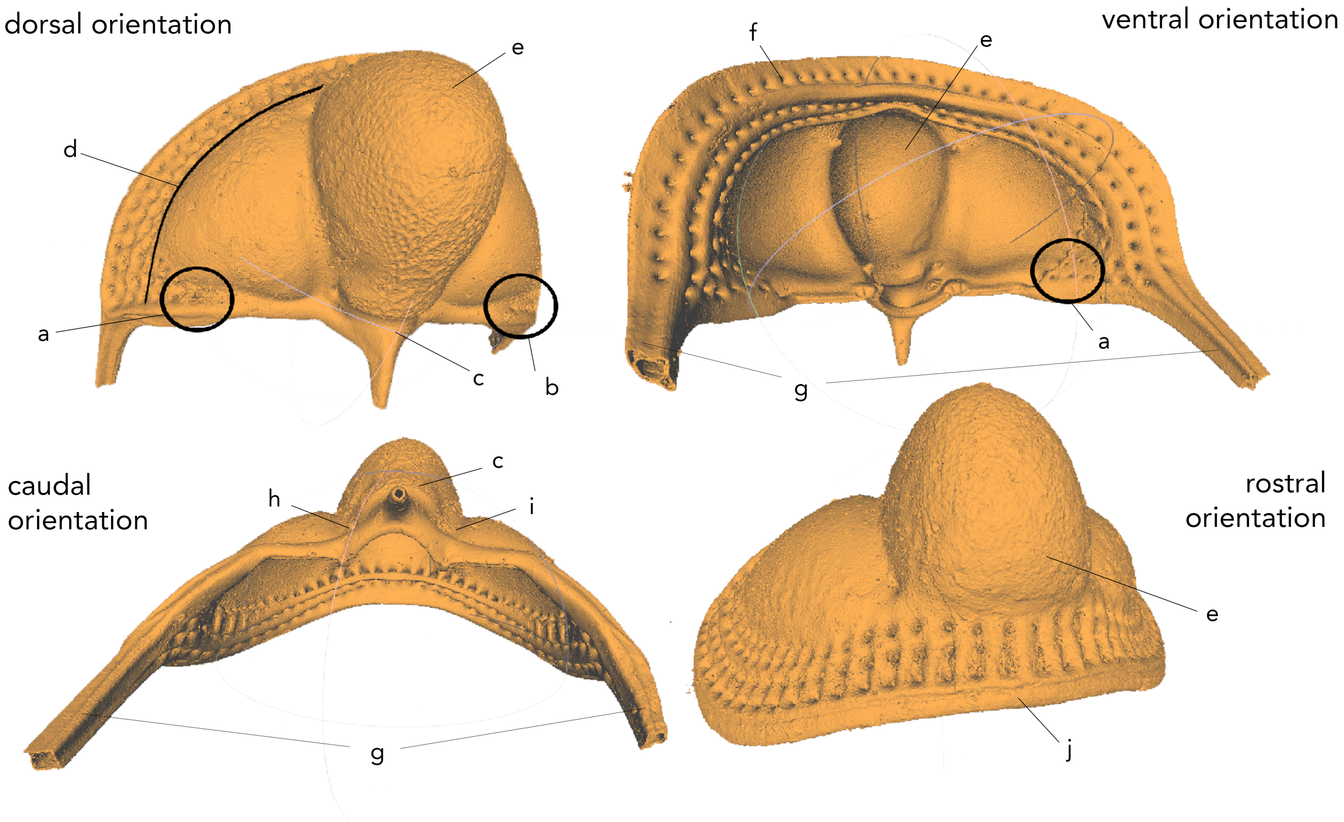

Fig VI: *C. tesselatus* anatomy based on a CT scan of an adult (late holaspid) specimen. Legend in Appendix I. (Image adapted from Hopkins and Pearson, 2016).

Paleoecology and Depositional Environment

An Ordovician outcrop notably rich in *C. tesselatus* fossils exists as part of the Kope Formation in northern Kentucky. The lower-middle Kope is characterized by of irregularly bedded argillaceous limestone that ranges from poorly to well-sorted packstones and grainstones (Tobin 1982). The beds that contain trilobites are all limestone, while the gray, calcareous shale layers are typically devoid of fossils (Davis and Cuffy 1998). The bases of most of the beds are composed of concave-down brachiopod valves, along with bryozoan colonies.

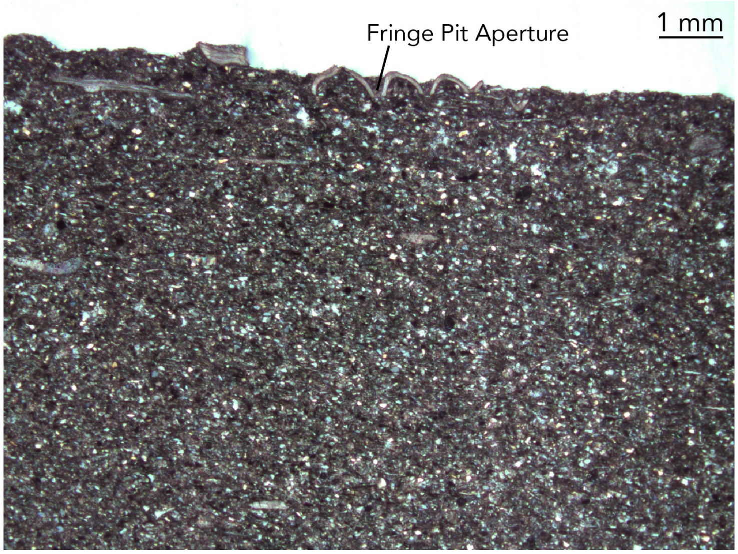

Fig VII: A vertical thin section taken from the lower-middle Kope Formation, showing fine grain indicative of a low-energy environment. The lower lamellum of a *C. tesselatus* fossil sits near the top of the section, with the aperture designated.

The Cincinnatian tends to demonstrate a stratigraphic record of alternating fossiliferous limestone with fossil-poor shales. This pattern has been attributed to shelly accumulations onto muddy seafloor via heavy storms (Bucher 1917). Since the late 1960s, the local depositional pattern is said to be the result of a quiet environment of muds and clays that would be interrupted by periodic storms. These interruptions, while rare, are the reasoning behind the significant number of concave-down brachiopod valves (Anstey and Fowler 1969). It has been posited that these brachiopods were the first to colonize the muddy environment. As the depositional environment became more stable due to brachiopod faunalization, trepostome bryozoans began to colonize the substrate, followed by crinoids, gastropods, and eventually trilobites (Harris and Martin 1979). The notable biodiversity of the colonizing species suggests a period of especially low energy deposition with the occasional storm.

Based on other studies of the Kope Formation, the habitat for this fauna would be on a carbonate ramp, far from shore, exhibiting fairly low energy, although still within the photic zone and storm-wave base (Brett and Algeo 2001). Limestone samples containing *C. tesselatus* were petrographically examined and can be characterized as well-sorted mudstones (Fig VII). The vast majority of the matrix averaged to .05 mm. The Hjulström curve, which correlates depositional grain sizes to necessary flow rate, suggests that these grains would have been deposited with a flow velocity of approximately 30 mm/s, and remain stable at current speeds up to around 25 cm/sec. While currents of such a high velocity would be rare in this depositional setting, overturned brachiopod valves are substantial evidence that they did in fact occur (Harris and Martin 1979).

Enrollment Behavior

The distribution of *C. tesselatus* fossils across the United States shows confinement to similar depositional settings, which indicates that their benthic environment was a constant. Trinucleids, in deep waters, were a rare order of trilobites that typically lacked eyes. Thus, their ability to visually locate food sources was limited, along with their ability to defend themselves against predators. Cephalopods, the dominant predators in Ordovician oceans, were notably dexterous, strong, and strategic hunters, making blind trilobites especially easy prey.

Due to the radiation of predators, most trilobites adopted flexible articulations of thoracic segments, allowing them to enroll. By contracting the cephalon and pygidium together, trilobites could rest in a defensive capsule that protected the organism's vulnerable underside. Many Ordovician specimens even exhibit coaptative, or geometrically paired, structures—cephala and pygidia that fit together like puzzle pieces. Through the contraction of thoracic segments, many organisms could remain hidden and locked inside their enrollment position until the threat had subsided. While the cephalon and pygidium of *C. tesselatus* do not appear to be coadaptive, the pronounced glabella and ample space under the cephalon suggest trinucleids were capable of such enrollment behavior. When enrolled, the genal spines would extend vertically in order to fend off encroaching predators.

Historical Background

Despite being first described in 1832, the morphology of trinucleids was largely ignored until the late 19th century. The first comprehensive notes on fringe pits date to 1895, in a landmark morphology paper on trinucleid form (Oehlert 1895). Upon dissecting along the suture that lies between the lamellae and parallel to the fringe, Oehlert noted the upper and lower lamellae (the two sheetlike plates that when placed together, form the fringe) were solid and did not need a communicating channel. Analogous structures have been described, suggesting the cephalon's robust construction might have been used as a head shield in order to strengthen and protect the trilobite's more vulnerable features (Reed 1916). These studies do not, however, offer any comprehensive function for the pits themselves. A short-lived hypothesis suggested the pits allowed for a lightening of the skeleton (Stormer, 1930), an idea that would not be mentioned again until the 1970s. In fact, an alternate theory by Begg (1944) proposed that trinucleid pits are furnished with a basal mamelon containing a small orifice in the center. That small opening led to the first proposition of the fringe as a sieve, claiming it to be "a great advantage in a benthos life of a muddy environment."

Part of the appeal of the Begg filter-feeding model is its variability. As the trilobite skidded across its benthic habitat, stray particulate matter would have been funneled into the exposed pits, eventually reaching the mouth. This remained the dominant theory through the 1960s despite the literature showing a wealth of anatomical differences across samples. Survey papers noted the modal number of pits in *C. tesselatus* changes with geographic locale that aligns with subspecies designations (Whittington 1968). Some trinucleids were even found bearing an *additional* row of pits. Despite the morphologic variability among subspecies, the function of the pits as a sieve was still generally assumed. A notable flaw with the Begg model is that the full set of pits is not complete until the late meraspid stage, in which the trilobite body is marked with two or more articulated segments (Hopkins and Pearson 2016). This indicates that the fringe would not have fully grown until the trilobite had reached mid-ontogeny. Given the vitality of a feeding mechanism, ontogenetic studies began to imply that juveniles would have had a large disadvantage at reaching sexual maturity without such a device.

The increased interest in trinucleid ontogeny led to multiple reconstructions of its appendages (Bergström 1972) and a reevaluation of their functional morphology. Bergström's reconstructions assumed that the shape of *Cryptolithus* facilitated plowing through superficial mud in search of food. This model is analogous to the modern horseshoe crab genus *Limulus*, which lives in a similar environment yet relies on a completely unrelated feeding strategy and can be hundreds of times larger than an adult *Cryptolithus*. In this scenario, for the trilobite to be able to feed on nutrient-rich sediment flowing through the pits, there would have been no mechanism to prevent fouling. Bergström postulates that if the fringe was for filter-feeding, it along with cephalic brim may have scaled off a space beneath the animal from the surroundings to prevent prey from escaping. Without such a structure, he considered the fringe "no longer suitable for filter-feeding." However, his reconstructions provided an excellent shape for an entirely new hypothesis—hiding. Given their small size and unfavorable position on the food chain, Bergström suggested that the fringe's large size and lightweight construction might have been used for burrowing. Citing a series of unearthed trackways (Osgood 1970), Bergström claimed its "shovel-like" construction upholds this behavior.

The filter-feeding hypothesis had a renaissance in the early 1970s, largely due to an effort to rethink trinucleids as epifaunal deposit feeders. Variable pit sizes were suggested to be "size selective" for grain types (Cisne 1973), with the body being part of a "trunk-limb" mechanism. Cisne argued that the brim functioned to divert the finest particles into the feeding current. Work by K.S.W. Campbell (1975) threw Osgood's trackways into skepticism and the "shovel" mechanism along with it. Such a mechanism would not require pits in the upper lamellae, and furthermore would likely produce some sort of fossilized evidence of fringe contact with sediment. Citing Stormer's (1930) effort, Campbell noted that a primary function of strengthening the fringe is unlikely due to the fact that the trilobite would rarely come into contact with forces capable of damaging an unsutured fringe. Likewise, noting the vulnerability of the area under the sutures, Campbell argued against anything related to hydrostatic protection. Much of this thinking also directly relates to the hourglass shape of the fringe pits, as Campbell believed such a shape is actually less beneficial for locomotion. Considering the interior of the hourglass is also made of calcite, the creation of additional pits requires more mineral mass. Thus, it was reasoned that fringe pits do not decrease the mass of the cephalon, as the fringe would be otherwise hollow. Trinucleids, thus, somehow evolved a mechanism that *increased* weight and bulkiness, counter-intuitively suggesting more pits means more mass. The advantage of the fringe, therefore, must have been able to provide a substantial benefit to the organism at risk of totally hindering its movement.

Studies of pit microstructure also began to dissuade anatomists from filter-feeding and circulation mechanisms. The shape hinted at the implausibility of circulation, given that the pits at their thinnest are still much larger than the tubes used for circulating fluids in the body cavity of *Cryptolithus*. Furthermore, feeding via oncoming current would suggest dense pit placement at the anterior of the organism, and not an even distribution around all sides. Additionally, the symmetrical shape of an hourglass hints that fluid would be entering and exiting the cephalon equally, which the rostral (from the anterior) feeding model ignores.

Largely in response to these issues, an in-depth reconstruction of the trinucleid feeding mechanisms ended up reshaping the model entirely (Fortey and Owens, 1999). Instead of passing current rostrally, Fortey and Owens instead claim that the cephalic chamber would intake current caudally (from the posterior), in direct opposition to Bergström's model. The authors claim that the pitted fringe is only found on trinucleids that have other criteria that support filter-feeding. *C. tesselatus* upholds the characteristics consistent with a trunk-limb feeding mechanism, as seen in contemporary arthropods—*L. simiaefacies*, a crustacean, is a particularly good model of this. The trilobite could lodge itself into muddy sediment and, using its genal spines, support a nested position while keeping the pygidium suspended (Fig VIII). Theoretically, its small legs could move water in a small channel towards the underside of the glabella, trapping necessary food particles in the chamber adjacent to the mouth. Fortey and Owens believe edible particles could have been sorted into the feeding chamber by the remaining limbs.

This model, as it was poised to do, eliminates many of the problems the rostral strategy exhibits. For example, it would have allowed the trilobite to consume sediment grains larger than the 100µm pit diameter and expel the water. It also would have prevented fouling from sediment pushed aside as *Cryptolithus* moved through a benthic environment. Most importantly, however, it provides a logical reason for the peripheral pit distribution around the fringe. As sediment would not have entered as the organism glided forward, the outermost pits would have facilitated an outward flow in a caudal model.

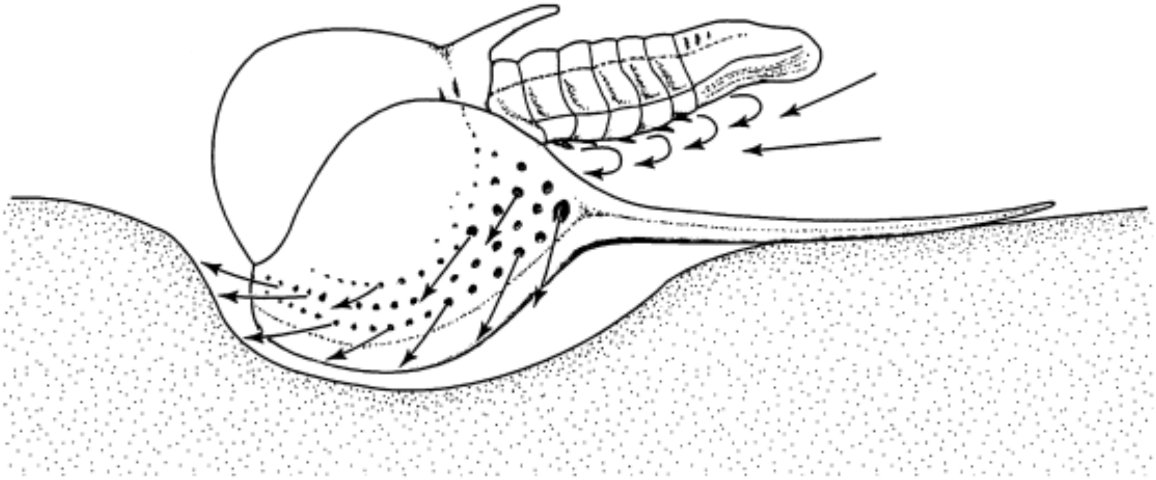

Fig VIII: Illustration of the Fortey-Owens caudal feeding strategy. (Image from Fortey and Owens, 1999).

The caudal feeding model, while certainly inventive, is not without its detractions. In the intervening years, several species in the trinucleid family have been described that have major sections of their fringe horizontally disposed, meaning that their pits are not positioned with the correct orientation to facilitate current through the fringe area (Whittard 1956). *Protolloydolithus*, for example, demonstrates that not all trinucleids shared the same pit layout. Some pits sat flush with the sediment and would have been be useless for such a task. These findings suggest that the caudal feeding model might not make sense for all trinucleids—an issue when the fringes are likely not analogous and not intended for the same function. Even when presuming all fringes were capable of expelling water in this fashion, the mechanism still lacks many basic features associated with efficient feeding techniques. Considering the vitality of feeding, it seems unparsimonious that such a complicated position in the sediment would have been required for relatively common nutrient consumption. This position also exposes the unarmored parts of the organism, making it incredibly easy prey. The model also offers no method of ridding the cephalic chamber of any unwanted particles too large to escape the fringe. Furthermore, the same pathways cited by Osgood, along with the few known fossils with pyritized limbs, indicate the exite fins were hardly paddle-shaped and instead brush-like. Thus, it is unlikely that the limbs could have been capable of creating water currents of sufficient magnitude for feeding purposes.

Testable Hypotheses

The fringe pits must have served a vital biophysical purpose given their prominence and retention through many species of trinucleids. Nonetheless, no extant hypotheses give reason for their hourglass shape. This project is, in part, an attempt at providing an experimental framework within which we can test the likelihood of several proposed hypotheses and derive a likely candidate that explains the reason for such an ornate design. Inferences on the trilobite's environment have been made based on a series of fossils collected from Kentucky's lower-middle Kope Formation. These inferences led to the design of models that are able to test function with best possible acuity.

The lack of consensus on the functional mechanism of the trinucleid fringe offers a unique opportunity for a study in experimental biomechanics. While no known analogs of any proposed mechanism exist in modern marine environments, the majority of these hypotheses rely on physical properties that can be reconstructed. Due to the interpretive nature of paleontology as a whole, a definitive answer cannot be reached. However, testability in these mechanisms might allow nuance into understanding issues with several proposed functions. Based on the literature review, we have proposed the following testable hypotheses.

- Filter-feeding (Rostral)

This test will evaluate the ability for flowing water to pass through the cephalon, and examine the viability for suspended particles to be consumed by the trilobite.

- Filter-feeding (Caudal)

This second test will look at the ability for the pits to allow caudal flow through the cephalon, supposedly to prevent pit clogging and fouling.

- Strengthening of Exoskeleton

This test will consider whether hourglass-shaped holes allow for a dispersion of stress, which potentially lowers the likelihood of the fringe to break in cases of deformation. Their shapes might hold a structural significance over other pit shapes, such as cylinders.

- Turbulence Reduction

Similar to a golf ball, the pitted fringe might be able to induce laminar flow over the cephalon, allowing the trilobite to maintain a firm stance on the ground and avoid inundation by oncoming current.

In developing a system of multiple working hypotheses, this project must take two important necessities into account. First, the cephalic fringe grows to its full size only by late meraspis. Therefore, juveniles must either have had no need for the function OR had an alternate mechanism. Secondarily, the outcome must provide a reason for the distinctive hourglass shape.

Methods: Filter-feeding and Circulation

In order to test the feasibility of water to carry food particles through the cephalic fringe, both a model of *C. tesselatus* and of its Ordovician ocean were created. A flume was constructed that was capable of ejecting laminar flow at a maximum plausible velocity for the habitat of *C. tesselatus*.

Construction of Flume

The HC1 is a custom-built hydrodynamic flume designed specifically for this experiment (Fig IX). The flume's plumbing and dimensions provide the optimal conditions for water to flow across a model organism with minimal edge effects and controlled flow velocity. The flume is constructed out of oak plywood and a single transparent plexiglass wall. It has a length of 150 cm, long enough for the flow to become laminar and dissipate behind the model; a height of 36 cm, allowing for a multitude of water depths; and a width of 36 cm, which can be 18 cm with a divider, allowing for a narrower channel and therefore, a faster flow rate.

Water is drawn from the downstream end of the flume through two 1" tubes that lead to two 1,000 GP submersible inline water pumps below the flume's base. The pumps direct water to the upstream of the flume, where flow progresses through a sheet of aquarium foam and a series of plastic baffles to reduce turbulence associated with water pumped into the flume channel. This facilitates the creation of natural, laminar flow around the trilobite model.

A depth of ten centimeters was chosen to optimize headroom above the model while also allowing for sufficient flow rates (Fig IX). Using the lateral divider in Figure IX and a depth of 10 cm, both pumps yielded a maximum flow rate of 18 centimeters/second. According to The Hjulström curve, this rate is generous compared with respect to moving the grain sizes associated with *C. tesselatus* deposits in Figure VII, and would best simulate deep-sea flow during a major storm. On the Hjulström diagram, 18cm/s falls on the boarder between depositing fine and medium sands and carrying all finer grain sizes in suspension. This likely exceeds the fair-weather living conditions based on grain sizes associated with the fossils. However, it is within the realistic range of what might be expected near the lower limit of wave action during a major storm. Also, because the goal was to test the feasibility that the pits facilitated flow in the cephalon, the experiment maximizes the likelihood for a positive outcome. Therefore, any inability to create flow through the pits in the model reduces the likelihood that any issues related to scaling could have demonstrated the outcome.

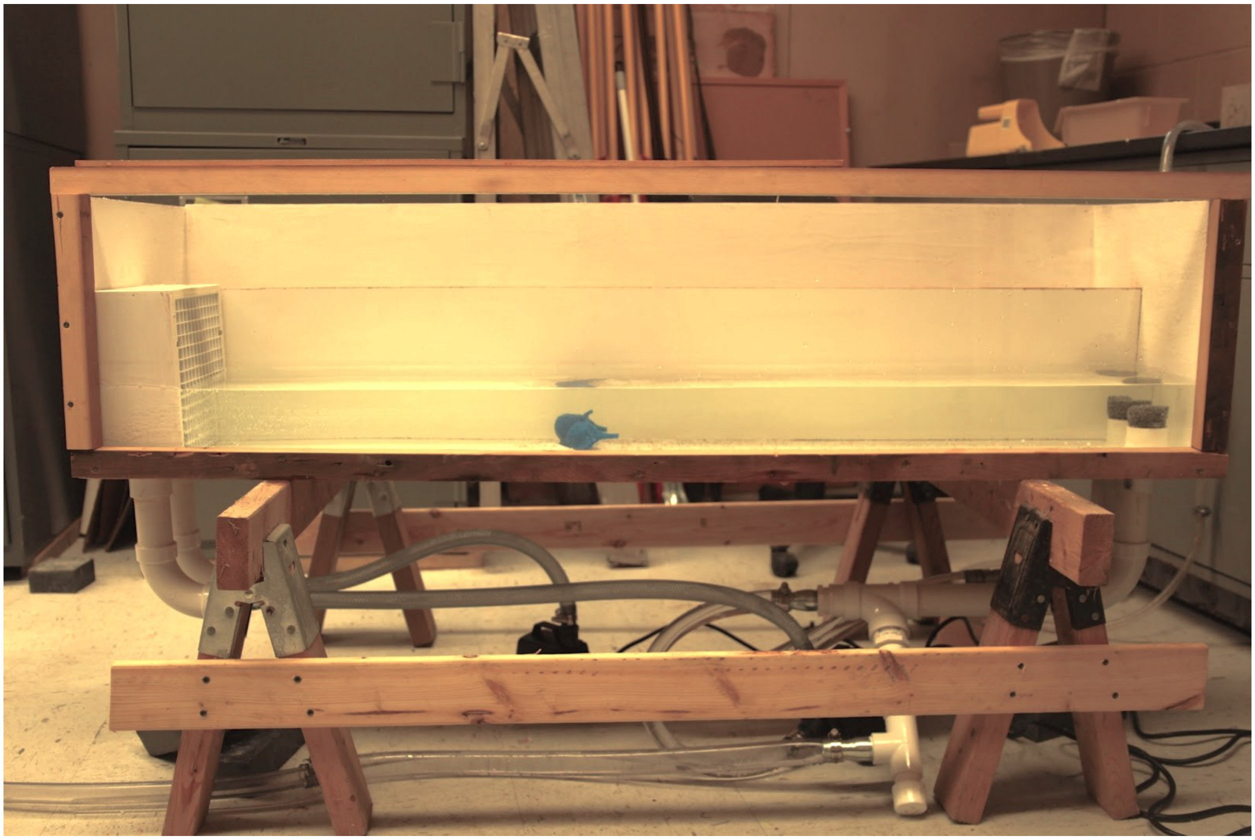

Fig IX: The HC1 hydraulic flume, specially designed for this experiment, used to assess flow around and through a model of *C. tesselatus* seed midway along the bed.

Choice of Model

Carrying out tests with an actual trilobite fossil proves difficult, as the vast majority cannot be removed from their sediment matrix without disarticulation. These fossils also tend to have occluded pits with infilled material that cannot be dissolved as the mineralogy of their body structure is calcareous, and therefore more vulnerable to dissolution or physical scraping than the shale that clogs the pores. Silicified specimens, while they exist, are rare and thus, cannot be subjected to many of the destructive or otherwise abrasive tests needed. Furthermore, the incredibly small size of *C. tesselatus* makes observing flow changes in flume tests rather difficult.

Given the difficulties with scale and media, our approach turned to creating a tenfold scale model of a late holaspid *C. tesselatus* by 3D printing a micro-CT scanned specimen (Hopkins and Pearson 2016). A silicified specimen was obtained from the invertebrate paleontology collection at the American Museum of Natural History (AMNH FL-81234). This collection is composed of residues from dissolution of a limestone sample (block M-1), collected by Marshall Kay from the Martinsberg Shale north of Spring Hill, Virginia. Given the similar sedimentary setting to the Kope formation, we are assuming that the site of burial in Spring Hill was quite similar to its natural habitat. Trilobite species obtained from dissolving the limestone block were previously described by Chatterton et al. (1990, 1994). Chatterton et al. (1994) also surmised that the samples were in rather close proximity to localities 11 or 12 of Whittington (1959).

CT Scanning

The specimen of *Cryptolithus tesselatus* was adhered to the inside lid of a small acrylic box or tube with Tragacanth gum, a water-soluble adhesive. The fossil was then scanned at the Microscopy and Imaging Facility at the American Museum of Natural History using a GE Phoenix v|tome|x scanner with 240kv microtube. Additional image post-processing and 3D surface rendering was done using VGStudioMax; and a surface model was exported as a polygon file (.ply).

Model Rendering

After scanning, the specimen was imported as a polygon file (.ply) into the open-source 3D computer graphics software Blender. As the scanned model's resolution was far too high for the printer's level of nuance, Blender was used to decimate the polygon file into one that could be

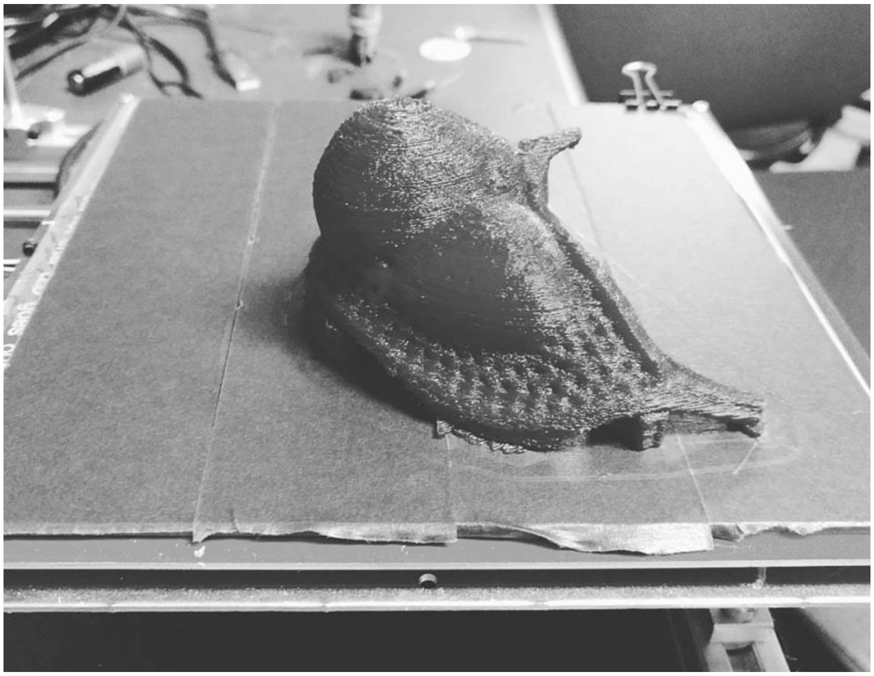

Fig X: The first 3D print model of *C. tesselatus* scaled tenfold.

printed efficiently. The model was then exported as an object file (.obj) and imported into the GCode generator program Slic3r. This program generates the quickest possible pathway for the printer nozzle to follow. Furthermore, using Slic3r allows for an algorithmic scaffold support structure to be generated; as the trilobite is large and convex, a support structure underneath the glabella is vital in case of collapse while the plastic is still warm and malleable.

3D Printing

The model was printed on a 2015 Watermelon printer using a plastic medium at the Oberlin College 3D printing lab. Each extruded layer of plastic sat at .175 mm thick and was ejected from a 2.85 mm nozzle. After printing, the models were broken off the printer bed and the support structures were removed (Fig X). As the model is based upon a high-definition CT scan, the internal structures of the *C. tesselatus* print are nearly identical to the scaled pyritized structure of the original specimen.

Even at its tenfold increased size, the fringe pits did not have openings that extended completely through the lamellae in the model. A 1/16” drill bit was used to complete the hole through the remaining plastic membrane.

Scaling

With a tenfold scale model of a holaspid *C. tesselatus*, the experimental conditions should ideally scale grain size of the surrounding sediments, flow rate, and fluid density. The scaling issues in this experiment (e.g., marginally larger-diameter pits, and using water rather than a more viscous scaled fluid to maintain Reynold’s number), therefore, maximizes the ease with which fluid should pass through the pits. Likewise, the model’s flow rate was higher than what might be expected in the interpreted environment of deposition for *C. tesselatus*.

To approximate the depositional setting, a small patch of sediment was placed underneath the trilobite, preventing excess water from flowing underneath. Melamine plastic was used, with grain size ranging from 0.4 to 1.4 mm, approximately ten times the size of grains in the fossil matrix (.05 mm, scaled to .5 mm). Scaling down to a tenth very closely correlates to the silt and clay sized particles found in the Kope fossil matrix. Using the Hjulström curve as a model, an appropriate velocity for the paleoecology of *C. tesselatus* in vivo would be around .3 cm/sec, indicating mostly stagnant water. For modeling purposes, this was scaled up to 18 cm/sec, six times the already tenfold measurement. Again, this biased the model in favor of the flow through the pits facilitating filter-feeding.

Test Protocol

Three videos were recorded for each orientation (rostral and caudal flow approach). The trilobite model was consistently placed midway across the flow channel and submerged in ten centimeters of water. A small amount of melamine plastic sediment was placed under the trilobite, as to both provide a realistic context for how the organism supposedly rested, and to ensure only trace amounts of water would be capable of flowing underneath the cephalic rim. Once maximum

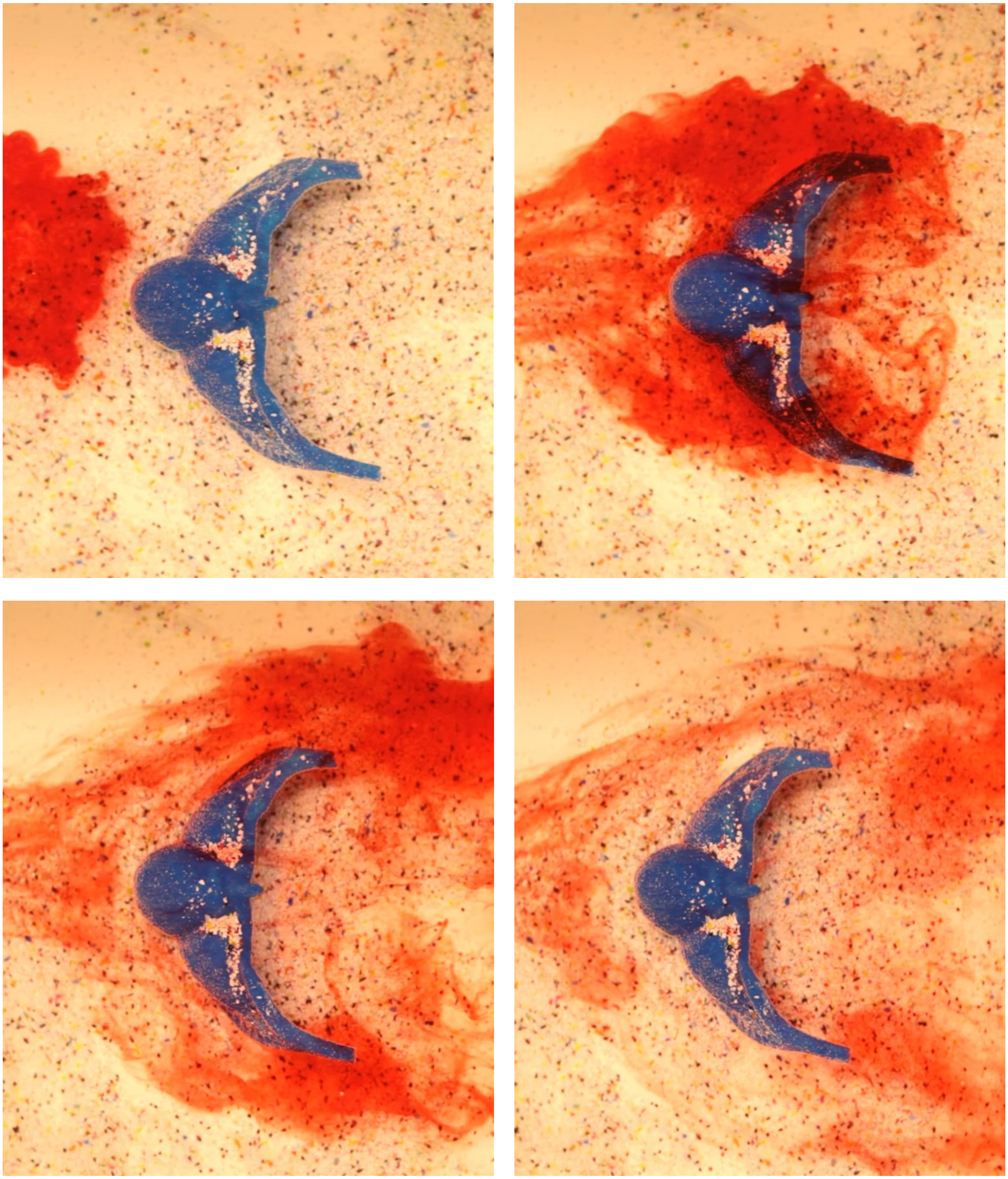

Fig XI: The rostral feeding test at a 50 cm injection distance photographed from above. Notice the dye's strong tendency to deflect around the fringe in oppose to going directly through it.

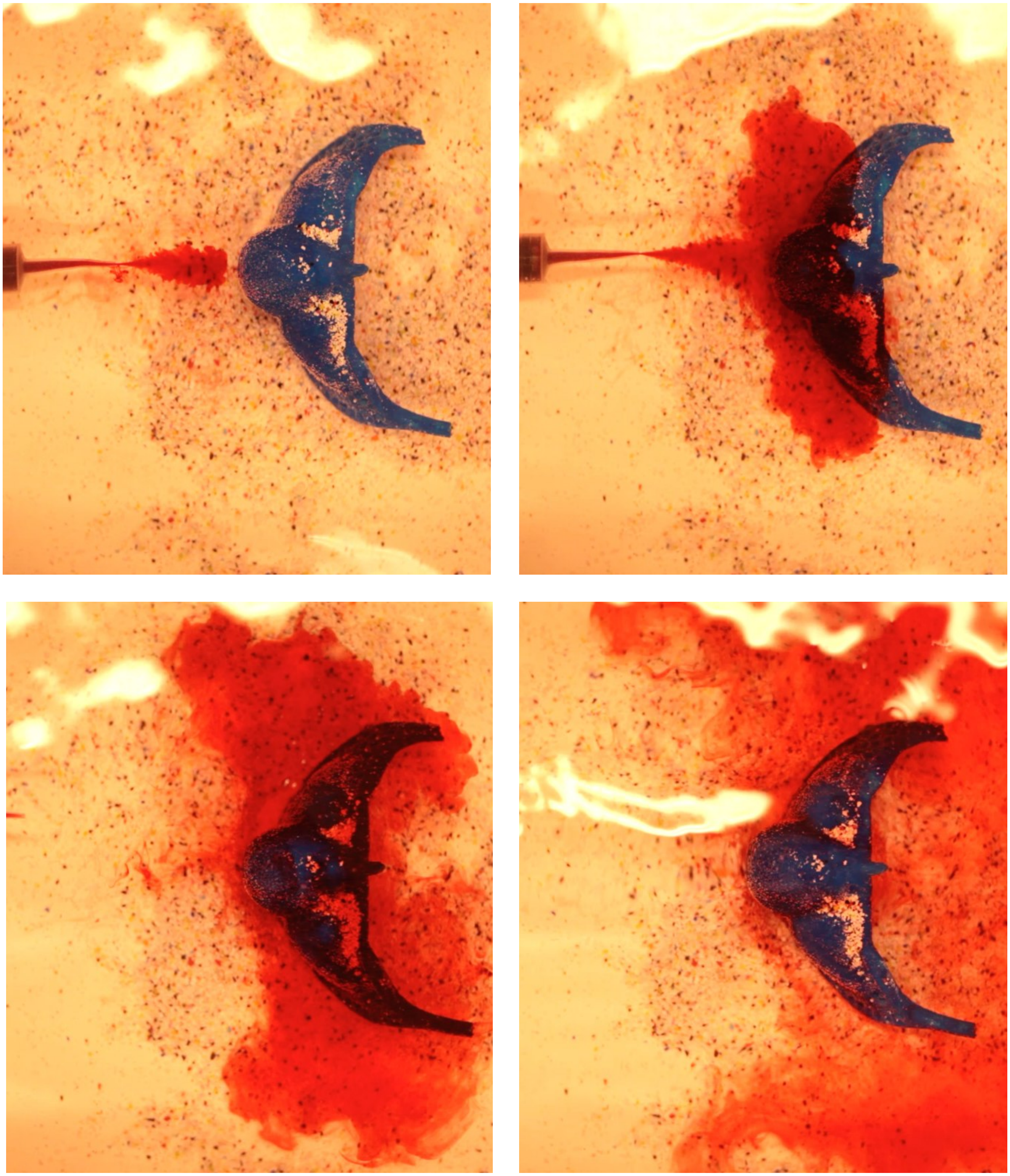

Fig XII: The rostral feeding test at a 5 cm injection distance.

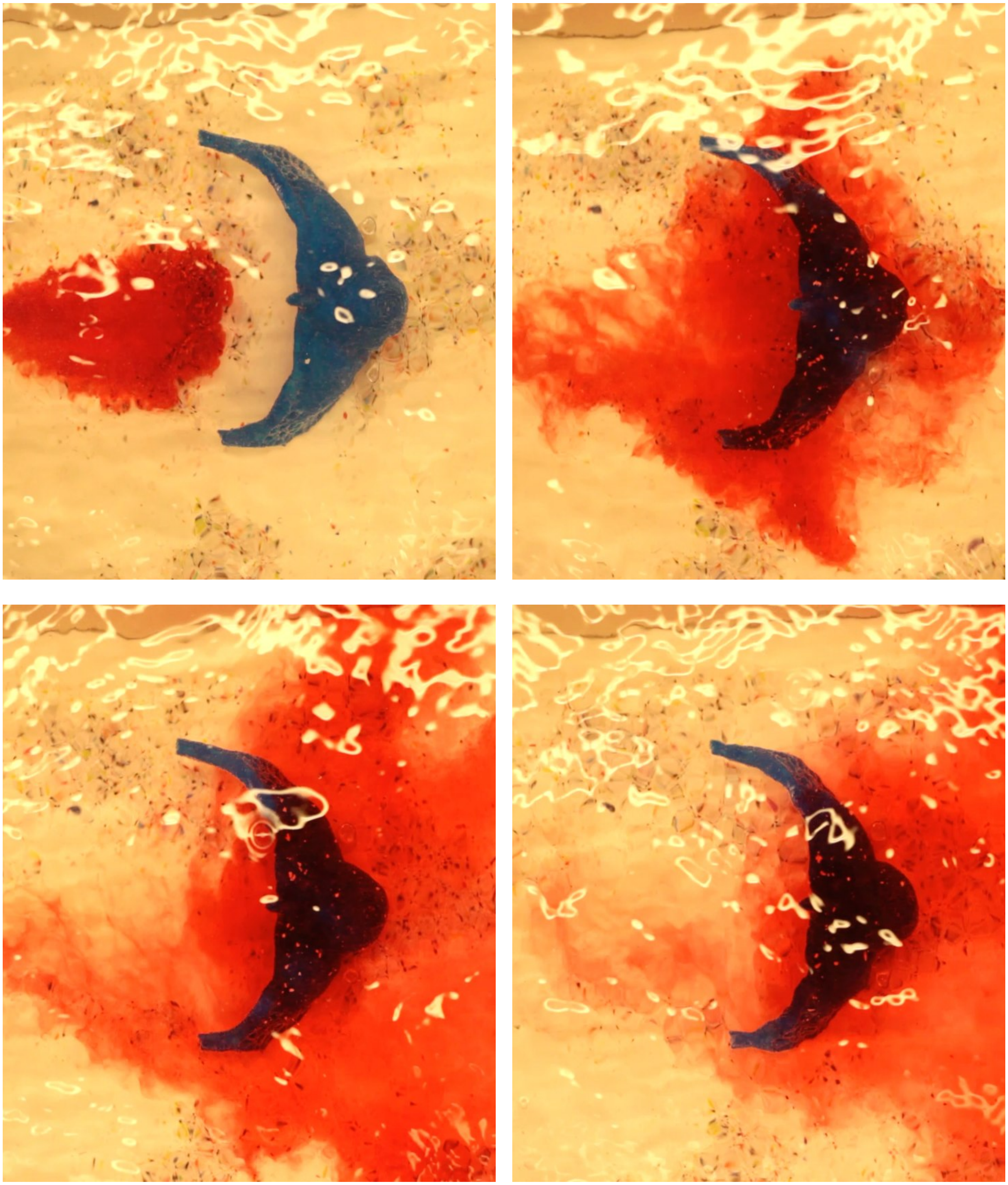

Figs XIII: The caudal feeding test at a 50 cm injection distance photographed from above. While considerably more dye passes through the fringe, the majority still pools beneath it.

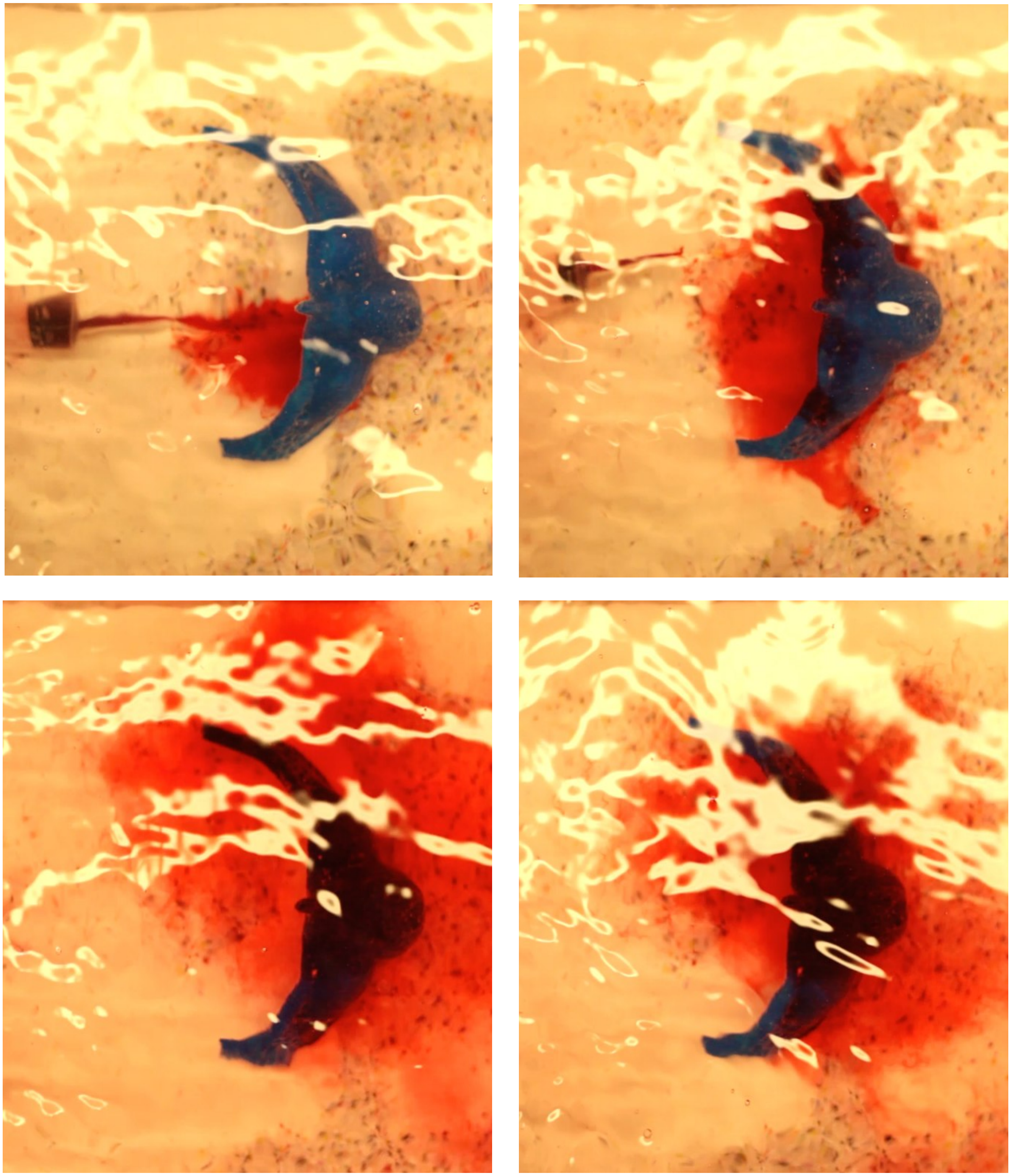

Fig XIV: The caudal feeding test at a 5 cm injection distance.

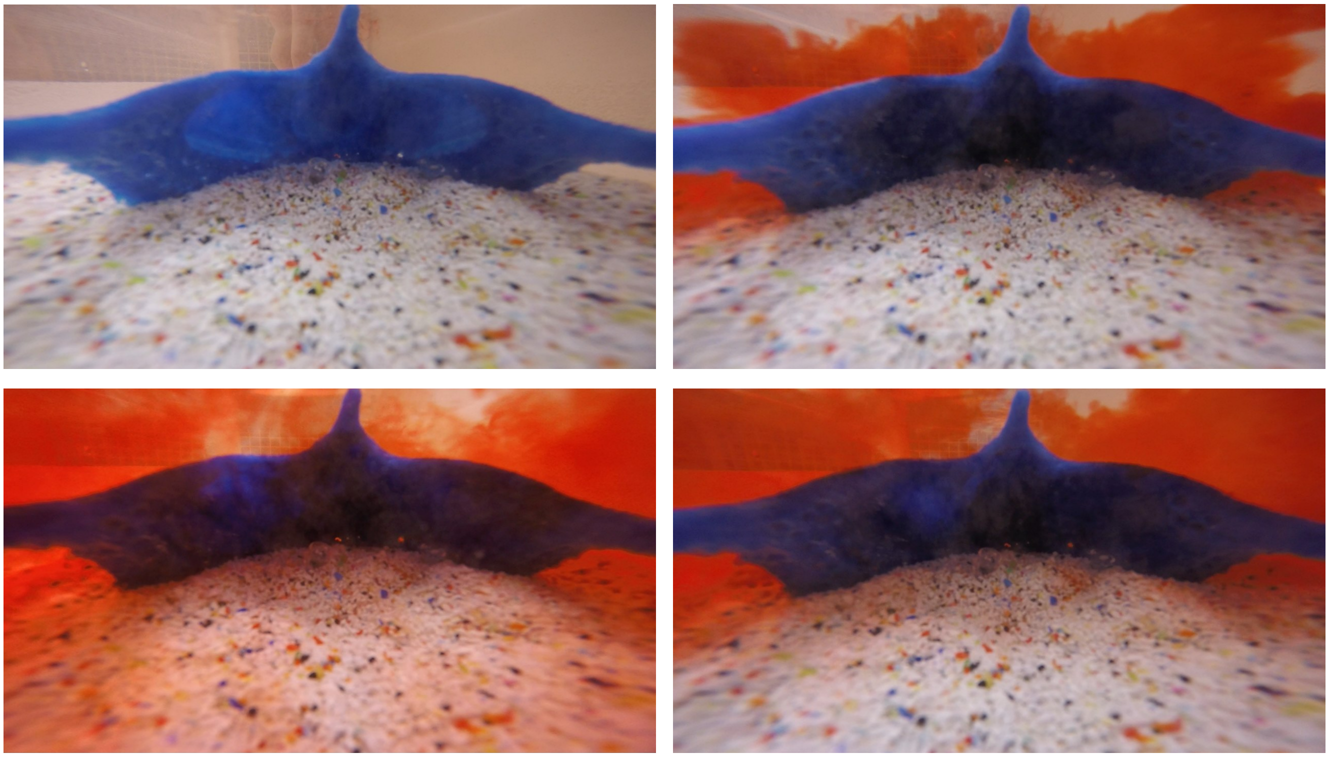

Fig XV: The rostral feeding test at a 50 cm injection distance photographed underwater, directly downstream of the trilobite model.

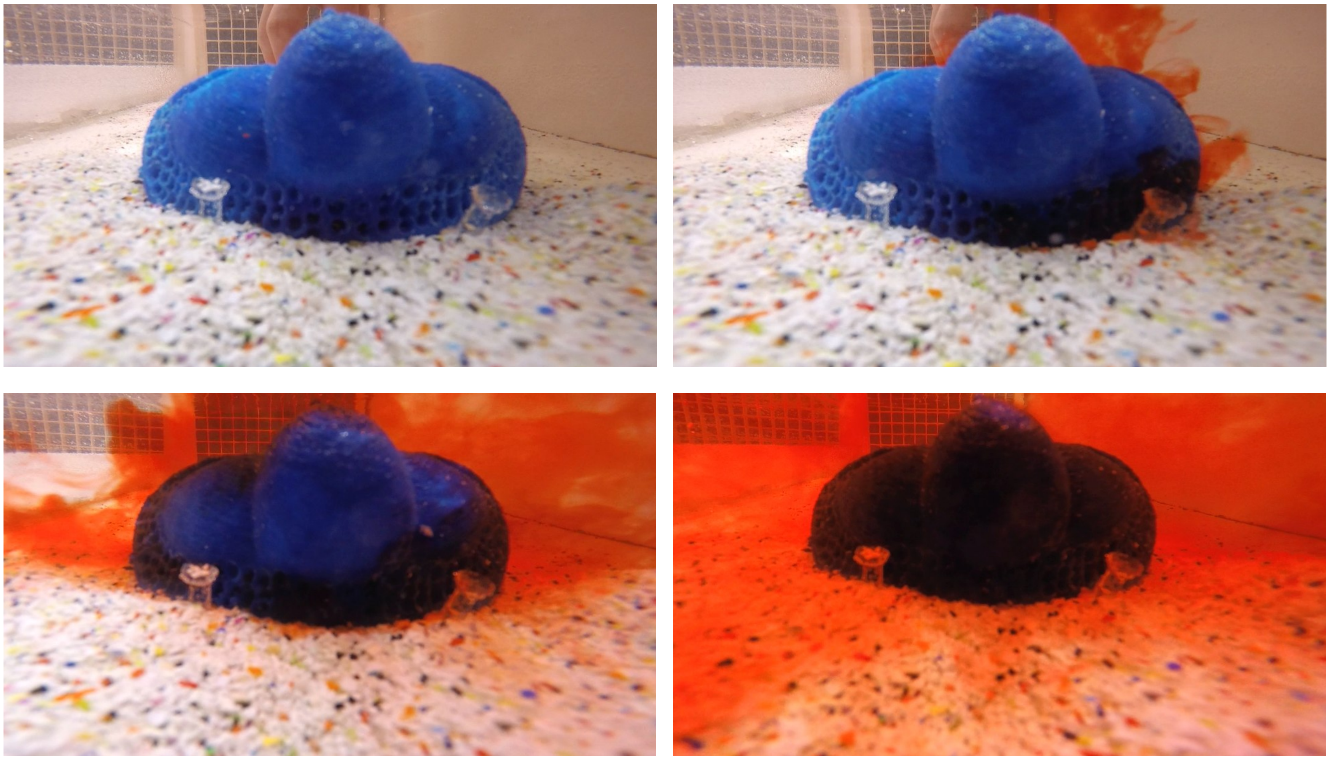

Fig XVI: The caudal feeding test at a 50 cm injection distance photographed underwater, directly downstream of the trilobite model. Note the clouding behind the cephalon with moderate amounts of dye moving through the underlying sediment, over, and around the cephalon.

flow was reached, 10 ml of red dye was injected into the flume from a point source immediately upstream from the cephalon.

The first video was recorded from directly above the model and red dye was introduced 50 cm upstream from the trilobite model (Figs XI and XIII). The second video is almost identical to the first, but with dye introduced five centimeters upstream from the trilobite (Figs XII and XIV). The final video was shot under conditions identical to the first video, but with the camera submerged downstream from the trilobite model to provide a second viewing angle (Figs XV and XVI).

Each test was filmed from directly overhead with a Canon Mark II DSLR and with a GoPro submerged downstream from the trilobite, both at a frame rate of 30 fps. Both orientations (rostral and caudal), from both camera angles, were sent to an anonymous group of thirty-six viewers in order to best characterize the amount of dye that successfully flowed through the fringe, as opposed to deflecting off or around it. Viewers were asked to estimate the amount of ink that was successfully "filtered" by the model and to separate that from the ink that bypassed the holes. Answers were multiple choice and quantized in intervals of 10%, with lower bounds from 0% to 50%. The cap of 50% was characterized by the experiment design team as a generous estimate after viewing the videos taken.

While clearly subjective, the use of a survey to quantify fluid amounts was considered to be the most accurate strategy for estimation. Given the erratic nature of the test and rapid dissipation of the red dye, computational methods proved to be very error prone and often displayed very clear flaws. While the videos themselves are also quite imperfect, they offer survey-takers the chance to watch and re-watch tests in order to develop a strong justification for their estimate.

Results: Filter-feeding and Circulation

The still photographs (Figs XI-XVI) show the progression of dye in each of the videos. Images are taken at 1-second intervals immediately after the dye's injection.

Figure XVII summarizes the perceived flow rates through the model pits based on thirty-six individual responses. The rostral feeding strategy had a significant trend towards the lower end of the spectrum, with 97% of respondents perceiving that under 30% of fluid successfully passed through. 86% of respondents claimed that less than 20% of fluid passed through from either direction. The observations suggest that the caudal test was more successful, with a much more scattered distribution. Over half of responses claimed that less than 20% of fluid successfully passed through the pits, yet a few responses expressed that a significant, though not a majority, of the fluid passed.

Analysis and Discussion: Filter-feeding

These results show that even when the viscosity of the fluid (water) is grossly reduced relative to the scale of the model specimen, the pits are scaled to greater than five times above the relative size of the organism, and current speeds are set higher than might be expected for the depositional setting, the fringe *still* does not allow enough fluid through to be considered a viable filter-feeding mechanism. The survey responses suggest that the fringe's ability to allow flow is ineffective at best.

From a biological perspective, the mechanism's limited success is further complicated by its sheer ecological cost. The extrusion of calcite is an energy-intensive task and is not likely to be carried out unless its absence would sincerely hinder the organism's daily functions. The metabolic rates required for such rapid growth and mineral sequestration are therefore, not likely attainable with the amount of nutrients that could pass through the fringe. Somewhat teleologically, its cumbersome size and shape cannot be supported by the proposed filtration function, nor can the requisite filtration be supported by its construction.

The practical reason for the lack of flow is the low fluid gradient on either side of the cephalon. While preliminary tests showed the gradient becomes more pronounced with higher flow velocities, the very fine-grained silts and clays that were typical of the trilobite's depositional environment reflect currents that would have been considerably lower than the scaled velocities used in this experiment. It is highly unlikely that currents of sufficient velocity would be a common occurrence in trinucleid habitat. It also seems unlikely that the fringe would be kept as a contingency mechanism in case a current of substantial velocity were to create the necessary gradient.

An additional piece of evidence against this hypothesis comes in the form of the horizontally disposed pits (Fig XVIII). As seen in other trinucleids, one of the lists of pits is situated

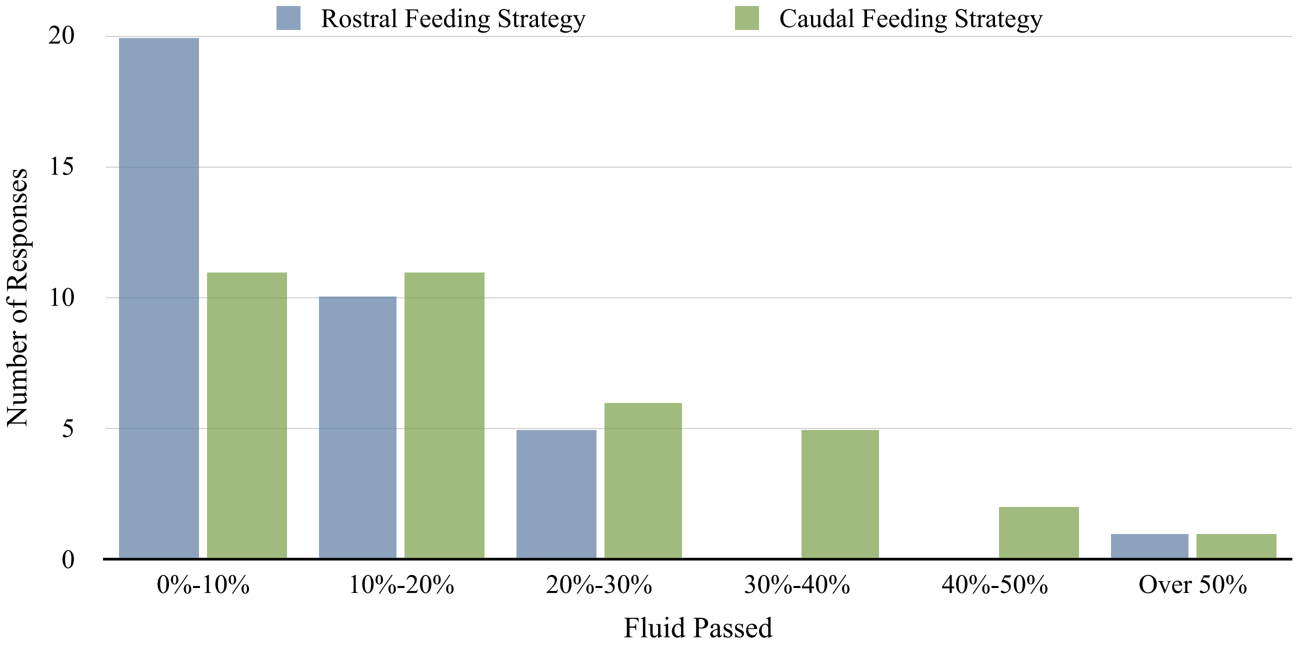

Fig XVII: Histograms that show the perceived amounts of fluid passing through the cephalon based on the approach direction of the flow. All observations suggest low success rates.

Fig XVIII: A ventral view of *C. tesselatus* showing the list of horizontal pits that would be flush with the sediment layer below. Scale bar in millimeters.

perpendicular to the primary lists, suggesting it would have sat flush with the sediment (Whittard 1956). Under the supposition that the pits were intended for passing fluid through, the inclusion of a list facing down into the sediment would be wholly unsuited for that purpose and renders the hypothesis less parsimonious.

It is worth noting that, in the experimental runs, the pits functioned as excellent traps for clay particles. Even with the limited amounts of sediment used during the experiment, filming was often hindered by particles lodging into the holes of the model. We reason that this would have been just as likely in its natural state (and perhaps exacerbated), given the highly cohesive clays that the fringe would have been actively plowing through. The hourglass shape, while tapered, offers no mechanism for sediment expulsion if trapped. It also limits the particle size of food to the smaller of the two apertures yet allows for larger grains to still clog the opening of the pit. Thus, in a benthic environment likely dominated by muds and fine sands, the pits seem to invite more sediment clogging than filtration. Given the vitality of a robust feeding mechanism, the propensity for clogging renders the fringe a poor tool for such a function—regardless of filtering direction.

The Fortey-Owens caudal feeding model, while slightly more successful than the Bergström rostral model, is still not without its issues. Primarily, the position needed for caudal filtration requires the trinucleid to wedge itself into the top layer of sediment while feeding. This poses problems, as feeding while in motion is not an option, and discrete feeding sessions must be regularly made. The general inefficiency of the fringe does not support this usage, which would need to allow considerably more sediment to permeate in order to be considered effective.

A further issue with caudal feeding is that the proposed strategy for inducing flow seems biologically unlikely. In the Fortey-Owens model, exite limbs would be able to stir the water column into a small current towards the back of the cephalon. However, the small number of known fossilized (pyritized) legs have an incredibly small surface area, suggesting their use as paddles would be quite limited (Raymond, 1920, Walcott, 1921). Fossilized trackways in sediment rich in *C. tesselatus* specimens resemble narrow lines rather than broad strokes, further illustrating that the ends of the appendages were more likely brush like (Osgood 1970). With such contingency on the legs to deliver sediment to the cephalon, the feeding mechanism seems too poorly constructed to have served the purpose for *Cryptolithus*.

Methods: Strengthening of Exoskeleton

Fig XIX: The shape of a three-minute glass game timer, an analog for the tapering pit shape on *C. tesselatus*.

While the filter-feeding test did not make use of the pit's hourglass tapering, the hypothesis of exoskeleton strengthening is contingent on it. Based on SEM imaging, the pits less resemble dimples on the outside of the fringe, but walls that comprise a networked systems of tunnels around the cranidium. This system of tubes might have allowed for a sturdy armature as the trilobite plowed through sediment as a deposit feeder without the unnecessary weight of a solid structure. While a fringe of solid calcite would indeed be durable, its sheer mass would have made locomotion especially difficult.

In order to test whether the hourglass shapes provided any structural advantage, we tested hourglass-shaped tubes against cylinders of the same radius. We hypothesized that one might expect a simple cylinder shape to be an ontogenetically simpler structure to create than the complicated hourglass shape. Therefore, we compared the durability of an hourglass against a cylinder to test whether the compressive strength increased enough to offset ecological costs.

Test Protocol

3D printing the hourglass shapes was ruled out as the printhead would have been unable to render them consistently in a form durable enough for testing. Three-minute glass timers (Fig XIX) with a diameter of 1 cm and an appropriately scaled aperture at the neck offered an approximate model for the distribution of stress that the fringe pits would also exhibit.

A series of seven glass timers were cut to 2.5 cm in height using a Beuhler Isomet Slow Speed mechanical saw with a wafering blade. The seven open-ended glass timers were arranged in a pattern with spacing proportionate to the distribution of pits on *C. tesselatus*. For comparison, seven additional cylinders were cut from the ends of the same glass timers in order to keep material specifications as similar as possible.

Both groups of seven were arranged in a clay bed in order to maintain stability. They were then submerged in the HC1 flume, so as to fill vesicles with fluid and to ensure equal internal and external pressure. They were then placed under a plexiglass sheet, so as to provide a platform for weights placed on top. A series of lead bricks were serially placed on the platform until the glass shattered and collapsed.

Results: Strengthening of Exoskeleton

Measurements of sustained weight were taken after each weight was placed on top, yielding a maximum weight that was successfully sustained and a second weigh associated with its breaking point.

	Weight Successfully Sustained (kg)	Breaking Point (kg)	Relative Strength
Hourglass Shape	18.14	21.07	1
Cylinder Shape	68.96	73.01	3.46

Analysis and Discussion: Strengthening of Exoskeleton

Results show that the cylinder shape was capable of sustaining over 3.4 times the weight of the hourglass, rendering the hourglass a much less sufficient shape for distributing stress across the cephalon. Thus, it is very unlikely that the hourglass was selected over a cylinder merely for reasons of greater compressive strength. However, given the many difficulties associated with growing cylindrical pits, we believe the shape might still be associated with cephalic structure. The inclusion of pits of any shape also creates a network of tubes that extend throughout the cephalon (Fig XX). The negative space around the pits forms a robust armature, giving the fringe significant depth and roundedness. This could serve as an optimized morphology between solid calcite—which would likely be too heavy, and cylindrical pits—which would be stronger and use less mineral, yet difficult to build.

General Discussion

Biological Analog: Insect Elytra

With the understanding that fluid likely could not pass through the fringe pits with enough efficiency to be used as a feeding structure, their use as a strengthening mechanism seems increasingly likely. While the shape does not offer the optimal dispersion of force, its shape offers some interesting interpretations.

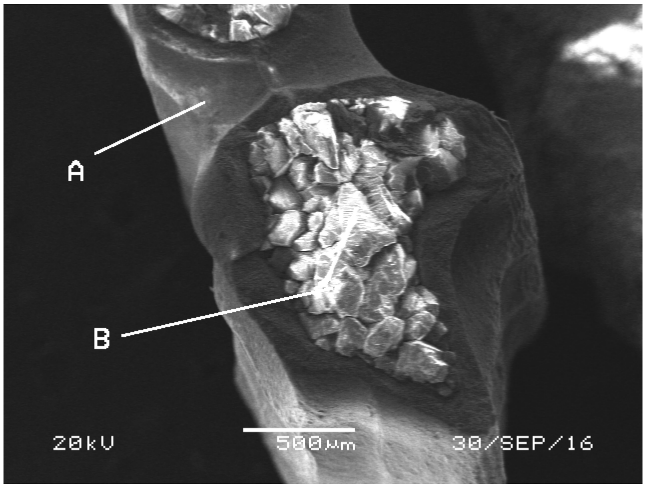

Fig XX: A cross sectional scan of the fringe of *C. tesselatus* indicating an hourglass fringe pit (A) and the networked series of tubes that make up the rest of the fringe. These tubes are presently filled with calcite (B), although they would have been fluid-filled in vivo.

Trabeculae, hollow chambers with a slight camber, are quite common in modern structural biology and tend to be used for strengthening. One of the best studied features exhibiting the cambered shape is the elytron—a hardened forewing found in many orders of insects. Elytra have been shown to be topologically distributed and can withstand coupling forces far greater than an unpitted wing (Dai 2010).

Elytra in insect wings bear a striking resemblance to the shape of fringe pits in trinucleids (Fig XXI), both in terms of the pit camber and the hollow tubes that extend around them. In beetles, the elytra's lightweight border structure allows for an optimized shape capable of withstanding isometric stress from all angles. Thus, the pit has fewer points of weakness than a cylinder would (He et. al 2015). For this reason, the hourglass shape has obvious advantages in engineering—a recent paper showed that hourglasses demonstrate only one mode of structural failure while cylindrical specimens were considerably more erratic (Bezerra et. al 2016). Finite element method analyses demonstrate that hourglasses concentrate stress near their center, an area in trinucleids that is buttressed by the suture. All this suggests that hourglass-shaped pits would have distributed force more uniformly between the two lamellae, rather than cylinders which would be less uniform. Thus, hourglasses may have represented the optimal shape to minimize the modes in which the fringe could deform.

Another possible interpretation of the hourglass shape is that, with little structural benefit, the shape is instead representative of a biological developmental constraint during trilobite ontogeny. As the amount of a particular chemical needed to biomineralize the cuticle is reduced, the pit shape changes trajectories from more columnar to more funneled. Arakane et. al (2012) noted that beetle elytra were formed with a delicate balance of two cuticular proteins, and that the relative amounts could change the elytra's steepness. The formation of trilobite trabeculae during

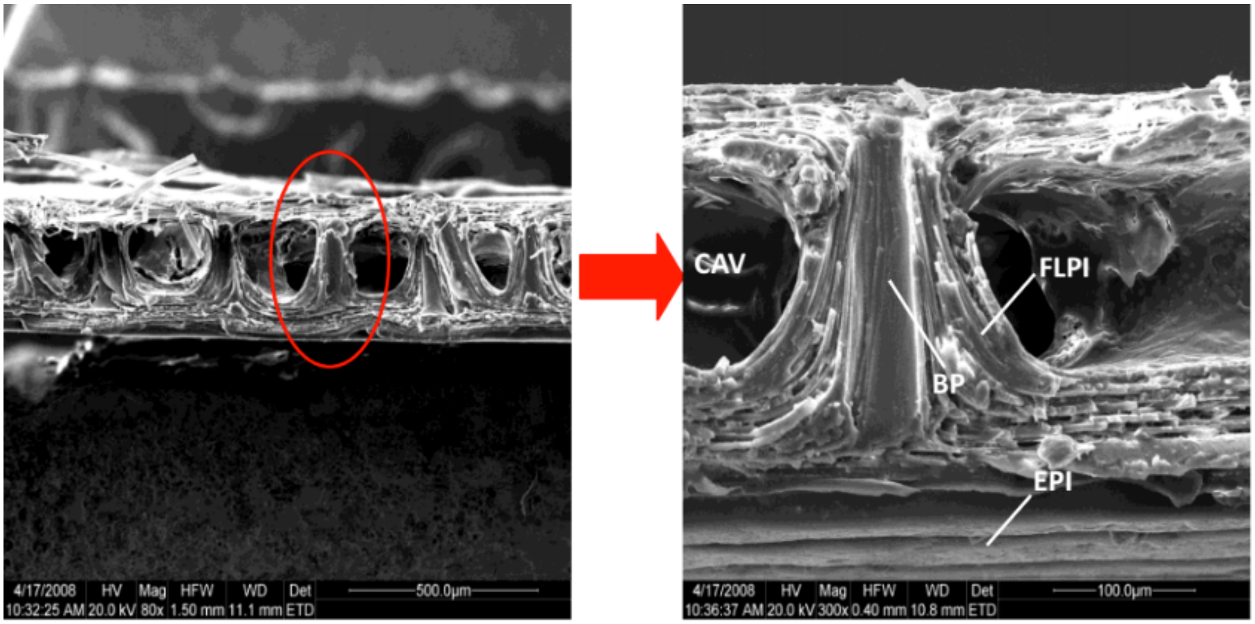

Fig XXI: A cross section SEM image showing beetle elytra microstructures. EPI, Epicuticle; FL, Fibre layers; CAV, Cavity. (Image from Guo et al. 2015) embryogenesis might have exhausted one such protein, which would have led the shape to begin its slow narrowing towards the suture.

A significant difference between the trilobite fringe pits and beetle elytra is their symmetry. In most modern insects, pits are found only on the external of the elytron and thus resemble a funnel much more than an hourglass. Presuming arthropod dimpling did not arise analogously between the *Trilobita* and *Insecta*, the developmental program used likely followed the same ontogenetic pathway. In *C. tesselatus,* for example, two complimentary pits could have occurred on either lamellum, and grew towards each other until they fused at their apices, producing the hourglass shape seen in the fringe. Presuming the morphogenetic program has remained similar across geologic time, growing pits that resembled columns would have been considerably more difficult, as the ratio of proteins would have to have stayed constant.

Topographic Interpretation: Catenoid

The shape of the fringe pit itself can most accurately be described as a catenoid, the rotation of a catenary curve around a central axis (Fig XXII). Catenoids are minimal surfaces, meaning they form a three dimensional shape with surface area when constrained by a closed space. The mean curvature of a catenoid is by definition zero, which means the shape can physically occupy the lowest possible energy state as it forms. Minimal surfaces are generally created in situations where surface tension becomes an important issue for the construction of form, such as dew drops. Catenaries, which form the “walls” of the catenoid, are commonly found in nature. A hanging chain, for instance, will form a catenary as it automatically distributes its weight to the point where it uniformly curves (Fig XXIII). Three dimensional catenoid shapes occur naturally as well. A common example is soap film attached to two identical rings. As the rings separate, the soap film will automatically taper inwards depending on its length. The catenoid shape ensures that the curve remains equally distributed across its length. The catenoid can be rendered by the parametric equations:

$$x = c\cosh\left(\tfrac{v}{c}\right)\cos u$$

$$y = c\cosh\left(\tfrac{v}{c}\right)\sin u$$

Where $u \in [0,2\pi]$

Thus, the catenoid has a mean curvature (H) of zero. In the physical world, having a zero H-value translates to shapes following an optimized energy function. Soap bubbles, like draped chains, follow a minimization principle in that their geometry always defaults to the lowest possible energy state. For a soap bubble, this lowest energy state is directly correlated with the smallest surface area, which is why free-floating bubbles form spheres.

A plausible reason for the catenoid specifically is that external forces might have been distributing the building material evenly during formation. As the fringe was likely composed of a somewhat flexible protein polysaccharide infused with carbonate, the growth of the fringe pits might have resulted from a process quite similar to the formation of catenoid soap bubbles. As the trabeculae begins elongation, epidermal cells are patterned around the fringe and begin to dimple inwards to meet the antithetical apex on the other lamellum. As the material thins, gravity and the tensile strength of the polysaccharide begin to warp until they reach a shape that approaches the minimal surface catenoid.

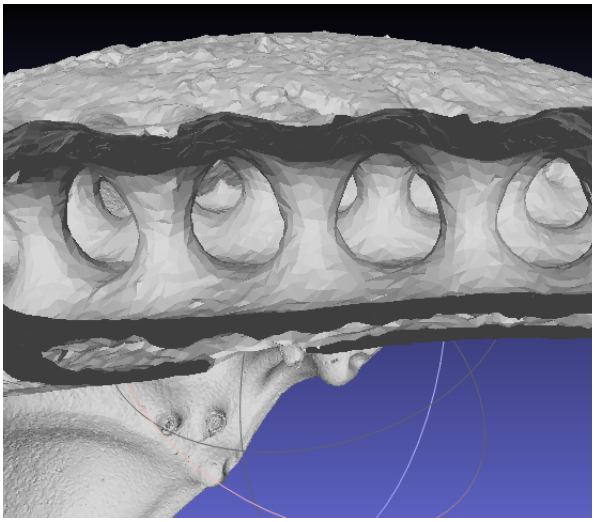

Fig XXII: The fringe pits as seen in a polygon rendering of *C. tesselatus*. Notice their catenoid shape.

Another potential advantage of the catenoid is not the pit shape it produces, but the shape of the negative space around it. Catenoids leave behind a rounded opening on all sides, which in turn also have a mean curvature of zero. At such small scales, minimal surfaces are much more efficient in resisting compression, in oppose to tension that we see at visible scales. Curved pits allow for a tubelike structural support system inside the fringe. This not only keeps the fringe much more lightweight than a solid fringe of calcite, but affords a larger surface area which would allow for the plowing of food particles and more efficient consumption of organic nutrients. While a cylinder would still be a stronger shape in itself, the space it leaves behind would be squared and therefore, a weaker lattice. Trinucleids, thus, are able to attain a large fringe because of the inclusion of this minimal surface lattice structure.

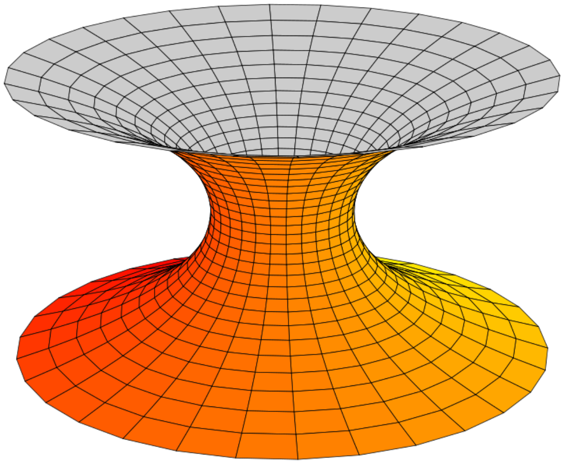

Fig XXIII: A catenoid, a minimal surface curved shape which can be used to describe both the fringe pit shape and potentially also its growth pattern.

Furthermore, the fringe pit honeycomb arrangement allows for a more efficient dispersal of stress than a checkered pattern would. As a checkered pattern allows for internal pressure on four sides, it has four possible ways of deforming. The tessellating fringe pits, however, disperse stress in three directions. This arrangement of alternating lists allows for the area between fringe pits to be especially secure.

Paleoecologic Implications

The catenoid shape, with the allowance of a stronger and rounded lattice structure, allows for a larger cephalon. A large ratio of cephalon to thorax allows for better protection from oncoming impurities as well as a simple armored plate in which the thorax and pygidium can curl under. Of course, many orders of Ordovician trilobites were evolutionarily successful without such wide cephalic fringe (Fig XXV). A short study was carried out in which the average cephalon to thorax ratio was calculated for fifty genera of Ordovician trilobites (Appendix C). The genera were then compiled and organized by depositional environment and ecology through the aggregate fossil database Fossilworks. The results (Fig. XXIV) show a strong correlation between paleoecology and cephalic ratio.

Paleoecology	No. Trilobites in Set	Average Ratio	Relationship
Reef, Buildup or Bioherm	4	0.936	microthoracic
Shallow Water Carbonates	11	0.969	microthoracic
Offshore Shelf	13	1.045	isothoracic
Peritidal	3	1.053	macrothoracic
Shallow Subtidal	7	1.136	macrothoracic
Deep Subtidal	12	1.356	macrothoracic

Fig XXIV: The average ratio for fifty genera of Ordovician trilobites, grouped by denoted paleoecology. Isothoracicism is defined as having a cephalon:thorax width ratio within the range of .95 to 1.05. Measurements were made without including genal spines as part of the cephalon and without legs as part of the thorax.

Typically, macrothoracicism correlates with trilobites found in lower-energy depositional environments, much like the paleoecology for trinucleids. This seems parsimonious, as a larger cephalon has the ability to clear a pathway with greater efficiency, especially through benthic muds and clays. This would continually provide a fresh layer of sediment to the area under the cephalon, where the trinucleid feeds from. Microthoracicism, on the other hand, tends to be associated with higher energy, shallow depositional environments where grain size is larger and more erratic. In the depositional survey for *C. tesselatus*, its paleoecology was likely poor in organic nutrients, given the green shales that surround it. A large cephalon, which promotes the removal of the topmost layer of clay, would allow trinucleids to skim a larger surface area with less movement. Large cephala also disperse force over a broader area, optimizing the necessary force to move sediment load. Thus, it is likely that larger cephala are to be selected for in lower energy depositional environments, and the addition of catenoid pits would promote a larger, more structurally sound cephalon.

Conclusion and Further Research

Given the highly inductive and often unconventional methods devised for functional morphology, drawing conclusions simply sets the stage for more rigorous experimentation. It

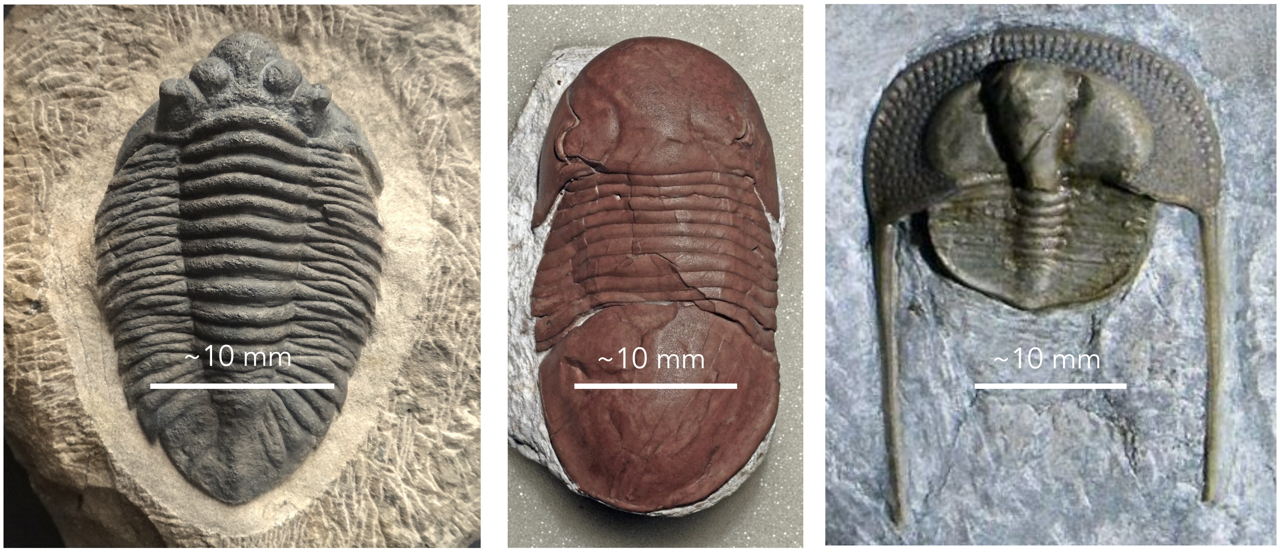

Fig XXV: From left to right, trilobite genera *Lichida*, *Failleana*, and *Cryptolithus* showing (respectively) microthoracicism, isothoracicism, and macrothoracicism. In general, macrothoracic trilobites—with a larger cephalon than thorax—are typically confined to benthic environments.

should be noted that many other inventive functions have been attributed to the fringe, although their methods are unfortunately untestable. Certain hypotheses, such as Campbell's creative idea that the pits were a sensory mechanism for water pressure, are unfalsifiable in a long-extinct species. Other such hypotheses include pit function as a digestive gland, or even a show for sexual selection. Although these inductive ideas promote inventive thinking and valid creative speculation, they are unfortunately untestable.

Using a combination of both model testing and comparative anatomy with beetles—a dependent group within the arthropod phylum—our study was able to produce a satisfying working hypothesis that suggests the trinucleid family behaved quite differently than previously expected. The conjunction of these methods suggests members of the family were deposit feeders that used a strengthened fringe for loosening food particles from surface sediments in a low-energy benthic environment. This offers substantial evidence against their current paleoecologic classification, epifaunal suspension feeders.

For these reasons, the major successes of this project were not so much in the conclusions drawn, but the methods used in order to disprove extant hypotheses. With two testable hypotheses for feeding, experimental design was rather simple and quite telling. The ability to cheaply produce a high-quality physical model allowed us to recontextualize already existing hypotheses and have a tangible representation of the fossil's morphologic function. Modeling based off high-resolution CT scans has shown to be fruitful, and its capability for digital distribution makes for a simple protocol in testing and retesting morphologic hypotheses. Furthermore, 3D printing allowed us to fabricate multiple models with slightly different morphologies, allowing us to digitally change morphologic variables and immediately test their impacts.

Despite its etymology as "the study of the ancient self," paleontology has spent the majority of its history confining the fossil record into very non-lifelike photographs. Compressing the narrative of life to two dimensions is somewhat taphonomic in itself, in that vast quantities of information are lost in rendering a 2D representation of 3D space. This lost material, which includes the fossil's orientation and spatial habits, happens to be vital for well-reasoned functional morphology. While 3D modeling of fossils is not a new phenomenon, the ability to rapidly disseminate designs, cheaply fabricate them, and slightly alter them for experimental purposes could finally bring digital functional morphology into the mainstream paleontology community.

As 3D rendering software continues to transition from CT scanning machines to consumer photography equipment, physical fossil modeling and testing will only become increasingly simple. The tactile abilities of a printed specimen allow for a much better understanding of its nuance, and challenge notions developed through traditional photography. Furthermore, the printer's ability to slightly alter morphology allows for intricate variables to finally be tested with simplicity. The future of paleontology will hopefully not only explore the past through photographic projections, but with accurate and mechanically reproducible 3D models. These technologies allow us to explore fossil evidence in a truly kinesthetic manner—tools that can make paleontology feel considerably more real, accessible, and provocative.

Acknowledgements

I would like to thank Dr. Karla Hubbard (paleontology) and Dr. Yolanda Cruz (developmental biology) for advising the project, and providing edits to both the test protocols as well as the paper itself. I would also like to thank Dr. Dennis Hubbard (sedimentology) for the design and construction of the HC1 flume. Dr. Melanie Hopkins (paleontology) of the American Museum of Natural History provided the CT scanned model and led the research project that inspired this study.

Additional research assistance was provided by Dr. Steven Wojtal (fluid dynamics), Dr. Susan Colley (mathematics), and Dr. Amy Margaris (physical anthropology) of Oberlin College, as well as Dr. Caleb Holyoke (materials engineering) of The University of Akron.

I would also like to thank Alexandra Kahn (entomology) for assistance with running tests and managing digital video, Henry Tobin (lab technician) for assistance with microscopy and CT scanning, the paleontology staff of the American Museum of Natural History for their technical support, Nigel McMillon (petrology) for manufacturing sediment thin sections, Ian Hunt-Isaak (computer science) for managing digital rendering software, and the Oberlin College 3D Printing Lab for assisting with model fabrication. The Oberlin College Geology Department Honors Program was managed by Dr. Amanda Schmidt.

Appendix I: Anatomy of *C. tesselatus*

Notable landmarks on the *C. tesselatus* cephalon. All of the following orientations describe a specimen with the anterior margin facing upwards unless otherwise specified.

a. F-pits, left side
b. F-pits, right side
c. Intersection of occipital furrow with sagittal axis
d. First internal list of fringe pits
e. Glabella
f. Horizontally-disposed list of pits
g. Genal spines
h. Posterior (caudal) apodome at edge tangent to axial furrow, left side
i. Posterior (caudal) apodome at edge tangent to axial furrow, right side
j. Intersection of suture between upper and lower lamellae and sagittal axis

Appendix II: Cephalon:Thorax Ratios on Fifty Ordovician Trilobite Genera

Trinucleids are bolded for simple reference. Isothoracicism is defined as having a cephalon:thorax width ratio within the range of .95 to 1.05. Measurements were made without including genal spines as part of the cephalon and without legs as part of the thorax.

Trilobite Genus	Order	Family	Cephalon: Thorax Width	Thoracic Habic	Depositional Environment	Ecology
Lichas Dalman 1827	Lichida	Lichidae	0.83	microthoracic	reef, buildup or bioherm	fast-moving low-level epifaunal carnivore
Hoplolichas Dames 1877	Lichida	Lichidae	0.85	microthoracic	carbonate	fast-moving low-level epifaunal carnivore
Allolichas Krueger 1992	Lichida	Lichidae	0.89	microthoracic	reef, buildup or bioherm	fast-moving low-level epifaunal carnivore
Pseudosphaerexochus Schmidt 1881	Phacopida	Cheiruridae	0.9	microthoracic	carbonate	fast-moving low-level epifaunal carnivore
Asaphopsoides Hupé 1953	Asaphida	Hungaiidae	0.9	microthoracic	offshore shelf	fast-moving low-level epifaunal deposit feeder

Trilobite Genus	Order	Family	Cephalon: Thorax Width	Thoracic Habic	Depositional Environment	Ecology
Eudolatites Delo 1935	Phacopida	Dalmanitidae	0.9	microthoracic	offshore shelf	fast-moving low-level epifaunal carnivore
Placoparina Whittard 1940	Phacopida	Cheiruridae	0.9	microthoracic	offshore shelf	fast-moving low-level epifaunal carnivore
Kanoshia Hintze 1952	Phacopida	Pliomeridae	0.90	microthoracic	peritidal	fast-moving low-level epifaunal carnivore
Eccoptochile Beyrich 1845	Phacopida	Cheiruridae	0.9	microthoracic	reef, buildup or bioherm	fast-moving low-level epifaunal carnivore
Ptyocephalus Agassiz 1843	Asaphida	Asaphidae	0.93	microthoracic	shallow subtidal	fast-moving low-level epifaunal deposit feeder
Plasiaspis Prantl and Pribyl 1949	Phacopida	Encrinuridae	0.96	isothoracic	offshore shelf	fast-moving low-level epifaunal carnivore
Lichakephalus Sdzuy 1955	Lichida	Lichakephalidae	0.96	isothoracic	peritidal	fast-moving low-level epifaunal carnivore
Pliomerops Billings 1859	Phacopida	Pilomeridae	1	isothoracic	carbonate	fast-moving low-level epifaunal carnivore
Atractopyge Hawle and Corda 1847	Phacopida	Encrinuridae	1	isothoracic	offshore shelf	fast-moving low-level epifaunal carnivore
Sokhretia Hupe 1956	Phacopida	Acastidae	1	isothoracic	offshore shelf	fast-moving low-level epifaunal carnivore
Ectillaenus Salter 1867	Corynexochida	Illaenidae	1	isothoracic	shallow subtidal	nektobenthic carnivore
Liomegalaspides Lu and Chang 1974	Asaphida	Asaphidae	1	isothoracic	shallow subtidal	fast-moving low-level epifaunal deposit feeder

Trilobite Genus	Order	Family	Cephalon: Thorax Width	Thoracic Habic	Depositional Environment	Ecology
Bumastoides Whittington 1954	Corynexochida	Illaenidae	1.04	isothoracic	carbonate	nektobenthic carnivore
Ptychopyge Angelin 1854	Asaphida	Asaphidae	1.05	isothoracic	shallow subtidal	fast-moving low-level epifaunal deposit feeder
Ceraurus (Eoceraurus) Esker, III 1964	Phacopida	Cheiruridae	1.1	isothoracic	carbonate	fast-moving low-level epifaunal carnivore
Diacanthaspis Whittington 1941	Lichida	Odontopleuridae	1.1	isothoracic	carbonate	fast-moving low-level epifaunal carnivore
Estoniops Eichwald 1858	Phacopida	Pterygometopidae	1.1	isothoracic	carbonate	fast-moving low-level epifaunal carnivore
Cyrtometopella Nikolaisen 1961	Phacopida	Cheiruridae	1.1	isothoracic	deep subtidal	fast-moving low-level epifaunal carnivore
Conocoryphe Hawle and Corda 1847	Ptychopariida	Conocoryphidae	1.1	isothoracic	offshore shelf	fast-moving low-level epifaunal carnivore
Eccoptochile Hawle and Corda 1847	Phacopida	Cheiruridae	1.1	isothoracic	offshore shelf	fast-moving low-level epifaunal carnivore
Ogyginus Raymond 1912	Asaphida	Asaphidae	1.1	isothoracic	offshore shelf	fast-moving low-level epifaunal deposit feeder
Trinucleoides Raymond 1917	Asaphida	Dionididae	1.1	isothoracic	offshore shelf	fast-moving low-level epifaunal deposit feeder
Bathycheilus Holub 1908	Phacopida	Bathycheilidae	1.12	macrothoracic	carbonate	fast-moving low-level epifaunal carnivore
Thaleops Conrad 1843	Corynexochida	Illaenidae	1.12	macrothoracic	carbonate	nektobenthic carnivore

Trilobite Genus	**Order**	**Family**	**Cephalon: Thorax Width**	**Thoracic Habic**	**Depositional Environment**	**Ecology**
Eobronteus Reed 1928	Corynexochida	Styginidae	1.125	macrothoracic	reef, buildup or bioherm	nektobenthic carnivore
Amphitryon Hawle and Corda 1874	Asaphida	Remopleurididae	1.13	macrothoracic	deep subtidal	nektobenthic deposit feeder
Omeipsis Kobayashi 1951	Asaphida	Taihungshaniidae	1.13	macrothoracic	offshore shelf	fast-moving low-level epifaunal deposit feeder
Hoekaspis Kobayashi 1937	Asaphida	Asaphidae	1.13	macrothoracic	shallow subtidal	fast-moving low-level epifaunal deposit feeder
Flexicalymene Roy 1941	Phacopida	Calymenidae	1.15	macrothoracic	carbonate	nektobenthic carnivore
Gabriceraurus Raymond and Barton 1913	Phacopida	Cheiruridae	1.2	macrothoracic	deep subtidal	fast-moving low-level epifaunal carnivore
Birmanites Sheng 1934	Asaphida	Asaphidae	1.2	macrothoracic	offshore shelf	fast-moving low-level epifaunal deposit feeder
Iberocoryphe Hammann 1977	Phacopida	Homalonotidae	1.2	macrothoracic	offshore shelf	fast-moving low-level epifaunal carnivore
Psilocephalina Hsu 1948	Asaphida	Asaphidae	1.24	macrothoracic	shallow subtidal	fast-moving low-level epifaunal deposit feeder
Raymondites Hall 1847	Proetida	Bathyuridae	1.28	macrothoracic	deep subtidal	fast-moving low-level epifaunal deposit feeder
Cheirurus (Cyrtometopus) Angelin 1854	Phacopida	Cheiruridae	1.3	macrothoracic	carbonate	fast-moving low-level epifaunal carnivore
Eoharpes Barrande 1872	Harpetida	Harpetidae	1.3	macrothoracic	deep subtidal	suspension feeder
Harpes Goldfuss 1839	Harpetida	Harpetidae	1.3	macrothoracic	deep subtidal	suspension feeder

Trilobite Genus	Order	Family	Cephalon: Thorax Width	Thoracic Habic	Depositional Environment	Ecology
***Marrolithus* Bancroft 1929**	**Asaphida**	**Trinucleidae**	**1.3**	**macrothoracic**	**deep subtidal**	**fast-moving low-level epifaunal suspension feeder**
Bathyurus Hall 1847	Proetida	Bathyuridae	1.3	macrothoracic	pertidal	fast-moving low-level epifaunal deposit feeder
Bufoceraurus Hessin 1989	Phacopida	Cheiruridae	1.46	macrothoracic	deep subtidal	fast-moving low-level epifaunal carnivore
Dolichoharpes Whittington 1949	Harpetida	Harpetidae	1.5	macrothoracic	deep subtidal	suspension feeder
Lioharpes Whittington 1950	Harpetida	Harpetidae	1.5	macrothoracic	deep subtidal	suspension feeder
Hibbertia Billings 1865	Harpetida	Harpetidae	1.6	macrothoracic	deep subtidal	suspension feeder
***Cryptolithus* Green 1832**	**Asaphida**	**Trinucleidae**	**1.6**	**macrothoracic**	**deep subtidal**	**fast-moving low-level epifaunal suspension feeder**
Asaphellus Callaway 1877	Asaphida	Asaphidae	1.6	macrothoracic	shallow subtidal	fast-moving low-level epifaunal deposit feeder

Works Cited

Anstey, R.L., and Fowler, M.L. (1969). Lithostratigraphy and depositional environment of the Eden Shale (Ordovician) in the tri-state area of Indiana, Kentucky, and Ohio: Journey of Geology, v. 77, p. 668-682.

Arakane, Y., Lomakin, J., Gehrke, S. H., Hiromasa, Y., Tomich, J. M., Muthukrishnan, S., ... & Kanost, M. R. (2012). Formation of rigid, non-flight forewings (elytra) of a beetle requires two major cuticular proteins. PLoS Genet, 8(4), e1002682.

Begg, J. L. (1944). On the fringe of tretaspis. Geological Magazine, 81(03), 113-117.

Bergström, J. (1972). Appendage morphology of trilobite cryptolithus and its implications. Lethaia, 5(1), 85-+.

Bezerra, U. T., ALVES, S., Barbosa, N. P., & Torres, S. M. (2016). Hourglass-shaped specimen: compressive strength of concrete and mortar (numerical and experimental analyses). Revista IBRACON de Estruturas e Materiais, 9(4), 510-524.

Brett, Carlton E., and Thomas J. Algeo. (2001). "Stratigraphy of the Upper Ordovician Kope Formation in its type area (northern Kentucky), including a revised nomenclature." Sequence, cycle and event stratigraphy of the Upper Ordovician and Silurian strata of the Cincinnati Arch region. Edited by TJ Algeo and CE Brett. Kentucky Geological Survey, University of Kentucky, Lexington, Kentucky: 47-64.

Bucher, W.H. (1917). Large current-ripples as indicators of paleogeography: Proceedings of the U.S. National Academy of Sciences, v. 3, p. 285-291.

Campbell, K.S.W. (1975). The functional morphology of cryptolithus. Fossils and Strata, 4, 65-86.

Chatterton, B.D.E., Edgecombe, G.D., Speyer, S.E., Hunt, A.S. and Fortey, R.A. (1994). Ontogeny and relationships of Trinucleodea (Trilobita). *Journal of Paleontology*, 68:523-540.

Chatterton, B.D.E., Siveter, D.J., Edgecombe, G.D. and Hunt, A.S. (1990). Larvae and relationships of the Calymenina (Trilobita). Journal of Paleontology, 64:255-277.

Cisne, J. L. (1973). Beecher's trilobite bed revisited: Ecology of an ordovician deepwater fauna. Peabody Museum, Yale University.

Dai, ZD and Yang, ZX. (2010) Macro-/micro-structures of elytra, mechanical properties of the biomaterial and the coupling strength between elytra in beetles. J Bionic Eng 2010; 7: 6 12–6 12.

Davis and Cuffey (1998). Sampling the Layer Cake that Isn't :: The Stratigraphy and Paleontology of the Type-Cincinnatian Issue 13 of Guidebook. Division of Geological Survey, Geological Society of America.

Delabroye, A., & Cronier, C. (2008). Ontogeny of an ordovician trinucleid (Trilobita) from armorica, france: A morphometric approach. Journal of Paleontology, 82(4), 800-810.

Fortey, R., & Owens, R. (1999). Feeding habits in trilobites. Palaeontology, 42(3), 429-465.

Harris, F.W., and Martin, W.D. (1979). Benthic community development in limestone beds of the Waynesville (upper Dillsboro) Formation (Cincinnatian Series, Upper Ordovician) of southeastern Indiana: Journal of Sedimentary Petrology, v. 49, p. 1295-1306.

He, C., Zu, Q., Chen, J., & Noori, M. N. (2015). A review of the mechanical properties of beetle elytra and development of the biomimetic honeycomb plates. Journal of Sandwich Structures & Materials, 17(4), 399-416.

Hopkins, Melanie J., and J. Kirk Pearson. (2016) "Non-linear ontogenetic shape change in Cryptolithus tesselatus (Trilobita) using three-dimensional geometric morphometrics." Palaeontologia Electronica 19.3 (2016): 1-54.

Green, J. (1832). A monograph of the trilobites of North America: with colored models of the species. Clark & Raser, Printers, Philadephia.

Oehlert, D.R. (1895). Sur les Trinucleus de l'Ouest de la France. Bulletins de la Societe Geologique de France, 23:299-335.

Osgood, R.G. 1970. Trace fossils of the Cincinnati area. *Palaeontographica Americana*, 6: 281-444.

Owen, A.W. (1980). A new species of cryptolithus (Trilobita) from the late ordovician of norway. Journal of Paleontology, 54(1), 144-148.

Raymond, P.E. (1920). The Appendages, Anatomy and Relationship of Trilobita. Mem. Conn. Acad. 4.

Reed, F.R.C. (1912). Notes on the genus Trinucleus: Geol. Mag., Dec. 5, v. 9, p. 346-353, pl. 1

Stormer, L., (1930). Scandinavian Trinucleidae, with special reference to Norwegian species and varieties: Norske vidensk.-akad. Oslo, Skrifta, I, Math. Nat. Kl., no 4.

Tobin, R.C., and Pryor, W.A. (1982). A model for cyclic deposition in the Cincinattian Series of southwestern Ohio, northern Kentucky, and southeastern Indiana: Ph.D. dissertation (unpub.), University of Cincinatti, 483 p.

Walcott, C.D. (1921). Notes on structure of Neolenus. Idem. 7.

Whittard, W. F. (1956). The Ordovician trilobites of the Shelve Inlier, west Shropshire. Part 2. Monograph of the Palaeontographical Society, 110 (473), 41–70, pls 5–9.

Whittington, H. (1968). Cryptolithus (Trilobita): Specific characters and occurrence in ordovician of eastern north america. Journal of Paleontology, , 702-714.

Whittington, H. (1959). Silicified Middle Ordovician trilobites: Remopleuridae, Trinucleidae, Raphiophoridae, Endymioniidae. *Bulletin of the Museum of Comparative Zoology*, 121.